



Article

Asymmetric Lévy Flights Are More Efficient in Random Search

Amin Padash ¹, Trifce Sandev ^{2,3,4,*}, Holger Kantz ¹, Ralf Metzler ³ and Aleksei V. Chechkin ^{3,5,6,*}

- ¹ Max Planck Institute for the Physics of Complex Systems, Nöthnitzer Straße 38, 01187 Dresden, Germany; padash@pks.mpg.de (A.P.); kantz@pks.mpg.de (H.K.)
- ² Research Center for Computer Science and Information Technologies, Macedonian Academy of Sciences and Arts, Bul. Krste Misirkov 2, 1000 Skopje, Macedonia
- ³ Institute of Physics & Astronomy, University of Potsdam, 14476 Potsdam, Germany; rmetzler@uni-potsdam.de
- ⁴ Institute of Physics, Faculty of Natural Sciences and Mathematics, Ss. Cyril and Methodius University, Arhimedova 3, 1000 Skopje, Macedonia
- ⁵ Hugo Steinhaus Center, Faculty of Pure and Applied Mathematics, Wrocław University of Science and Technology, Wyspińskiego 27, 50-370 Wrocław, Poland
- ⁶ Akhiezer Institute for Theoretical Physics National Science Center “Kharkiv Institute of Physics and Technology”, Akademichna 1, 61108 Kharkiv, Ukraine
- * Correspondence: trifce.sandev@manu.edu.mk (T.S.); chechkin@uni-potsdam.de (A.V.C.)

Abstract: We study the first-arrival (first-hitting) dynamics and efficiency of a one-dimensional random search model performing asymmetric Lévy flights by leveraging the Fokker–Planck equation with a δ -sink and an asymmetric space-fractional derivative operator with stable index α and asymmetry (skewness) parameter β . We find exact analytical results for the probability density of first-arrival times and the search efficiency, and we analyse their behaviour within the limits of short and long times. We find that when the starting point of the searcher is to the right of the target, random search by Brownian motion is more efficient than Lévy flights with $\beta \leq 0$ (with a rightward bias) for short initial distances, while for $\beta > 0$ (with a leftward bias) Lévy flights with $\alpha \rightarrow 1$ are more efficient. When increasing the initial distance of the searcher to the target, Lévy flight search (except for $\alpha = 1$ with $\beta = 0$) is more efficient than the Brownian search. Moreover, the asymmetry in jumps leads to essentially higher efficiency of the Lévy search compared to symmetric Lévy flights at both short and long distances, and the effect is more pronounced for stable indices α close to unity.

Keywords: asymmetric Lévy flights; first-arrival density; search efficiency



Citation: Padash, A.; Sandev, T.; Kantz, H.; Metzler, R.; Chechkin, A.V. Asymmetric Lévy Flights Are More Efficient in Random Search. *Fractal Fract.* **2022**, *6*, 260. <https://doi.org/10.3390/fractalfract6050260>

Academic Editor: Dumitru Baleanu

Received: 11 March 2022

Accepted: 30 April 2022

Published: 8 May 2022

Publisher's Note: MDPI stays neutral with regard to jurisdictional claims in published maps and institutional affiliations.



Copyright: © 2022 by the authors. Licensee MDPI, Basel, Switzerland. This article is an open access article distributed under the terms and conditions of the Creative Commons Attribution (CC BY) license (<https://creativecommons.org/licenses/by/4.0/>).

1. Introduction

Search strategies, in general, and random search processes, in particular, have recently attracted interest among scientists and practitioners who seek to understand food search strategies of animals [1,2] and diffusion control of molecular processes in biological cells [3], or aim at improving the performance of computer search algorithms [4,5] and optimise search processes for military tasks (hunting for submarines, locating enemy vessels and mines) [6,7]. In the concept of random search, the searcher has no prior knowledge about the location of its target and performs a random walk until it encounters the target—this process is called saltatory motion or blind search in the ecology literature [8]. In foraging theory, this saltatory search is distinguished from cruise search, in which the searcher looks out for targets (i.e., resource patches, mates, etc.) during its movements [9,10]. An essential part of all these processes and applications are various forms of random walk models, continuous or discrete in time.

The first studies on random search considered Brownian motion of the searcher as a default strategy. A prominent early example, motivated by his contact with the malaria researcher Ross, is Pearson's idea of a drunken man performing a “random walk” on the street grid of a city as a model for the spreading of malaria by mosquitoes in previously

non-infested areas [11]. Later, Shlesinger and Klafter proposed that Lévy motions with a scale-free, power-law distribution of jump lengths, represent a much more efficient strategy than the standard random walk or (in the continuum limit) Brownian motion, in the search for sufficiently sparse targets. Indeed, this higher efficiency is due to the combination of the thorough local search with occasional long excursions and hence the exploration of previously unvisited areas, thereby reducing the tendency towards “oversampling” of Brownian motion in one and two spatial dimensions [12]. The works on Lévy flight search of albatrosses [13], and on the general optimality of Lévy search [1], have attracted broad attention of researchers in the field of animal motility patterns and optimal search strategies. Viswanathan and colleagues [1,14], in particular, proposed superdiffusive Lévy flights as an optimal search strategy when searching for sparse targets in their “Lévy flight hypothesis”.

For the random search processes based on the Lévy flight model, the distribution of displacement lengths $|x|$ has the asymptotic power-law form $\lambda(x) \simeq |x|^{-1-\alpha}$ with $0 < \alpha < 2$ for which the second moment of the jump lengths diverges, i.e., $\langle x^2(t) \rangle \rightarrow \infty$ [15]. The resulting motion is spatially scale-free, and fractional, q th-order moments $\langle |x|^q(t) \rangle$ with $0 < q < \alpha$ exist. Lévy flights have found various applications, ranging from the famous flight of the albatross [13], spreading of spider-monkeys [16], grazing patterns of bacteria [17], over economical data [18,19] to molecular collisions [20], plasmas [21–23] and lattice gas automata [24,25]. In recent years, the search processes that optimise random blind searches for sparse targets in different settings have been discussed [9,26,27]. In particular, combinations of Brownian search and Lévy flights were studied [28].

In the last decade, other random search processes have been also proposed as alternatives to Lévy flights and have attracted considerable attention in the scientific community. Such models include intermittent dynamics that switch between local Brownian search events and ballistic relocation phases [29,30], for which the relocation time probability density may also be of the power-law form [27,31]. The intermittent strategy minimises the search time [32], and, for instance, is observed for the dinoflagellate *Oxyrrhis marina* when it preys on a microzooplankton [33], as well as for Nahua mushroom gatherers [34] following the so-called area-restricted search strategy [35]. In computer science and data mining (information retrieval) [36] one particularly popular search method is based on a random walk model, in which a combination of local and long-range searches is implemented, while in complex network theory, the calculation of the mean first-passage time of a searcher to find the target on a given complex networks is of high importance [37,38] for the description of a large number of real-world phenomena. Lévy flights have been promoted as a preferred strategy when there is insufficient prior knowledge on the search space. In particular, for sufficiently sparse targets, several analyses claim that the optimal value for the power-law exponent is $\alpha = 1$ [13,27,39,40], so that the jump lengths are distributed according to the Cauchy law. The central advantage of the Lévy flight’s strategy in comparison with the other strategies is its robustness: while other models work best when their parameters are optimised for specific environmental conditions such as the target density, Lévy flights remain close to optimal even when these conditions are altered [27]. Random search processes based on Lévy flights in the presence of an external drift (underwater current, atmospheric wind, a preference of the walker owing to prior experience or a general bias in an abstract search space), have also attracted attention in recent years [28].

From the mathematical point of view, the problem of calculating the first-hitting or first-arrival time of a point or an interval in the class of stable processes was the subject of several studies. We mention studies of the first-hitting time density of symmetric stable processes [41–49] and spectrally positive stable process [50,51] in which the authors obtained series expressions for the first-hitting density. Moreover, for asymmetric stable processes, with the help of the Lamperti–Kiu representation of self-similar Markov processes, the Mellin transform of the first-hitting time and a series expression for the first-hitting time density was obtained [52]. With the use of space-fractional Fokker–Planck equations, the first-hitting problems of symmetric Lévy flights and combined Lévy–Brownian motions

were studied [9,28,53–57]. This method is also employed in the present paper to study the first-hitting dynamics of asymmetric Lévy flights. Another method based on the Langevin equation, known as the simulated annealing algorithm, which is a semi-local search consisting of occasional long jumps based on the Cauchy distribution and Lévy stable laws, was studied in [58–60], respectively. Moreover, the first-passage problem of symmetric and asymmetric Lévy flights was studied by leveraging the Skorokhod theorem, and the analytical results were confirmed by extensive numerical simulations based on the numerical solutions of space-fractional Fokker–Planck equation and stochastic Langevin equations [61–64]. We finally note studies of the related problem of barrier crossing of Lévy flights [65–71].

By providing analytical and numerical investigations of random search based on asymmetric Lévy flights, we here aim at understanding this search strategy by analysis of the first-arrival time, the reliability and the efficiency. We seek to clarify under which conditions this type of asymmetric motion optimises random search. This will be achieved by investigation of both the (deterministic) Fokker–Planck equation with a δ -sink and the associated (stochastic) Langevin equation. The structure of the paper is as follows. In Section 2, we define the process of asymmetric Lévy flight search and compute the first-arrival density in terms of Fox H -functions. We provide a detailed analysis of the asymptotic behaviour of the first-arrival density in the short and long time limits. In Section 3, the analytical results are confirmed by numerical use of the Langevin equation for asymmetric Lévy flights. We also obtain the search efficiency and compare it with the corresponding efficiencies for Brownian and Lévy search in Section 4. The Summary is provided in Section 5. Details of the definition of α -stable processes, the definition and properties of the Fox H -function, as well as technical details of derivations are presented in the Appendices A–G.

2. Formulation of the Problem and Solution

We consider a space-fractional Fokker–Planck equation of the form:

$$\frac{\partial}{\partial t} f(x, t) = K_\alpha {}_x D_\alpha^\beta f(x, t) - \wp_{fa}(t) \delta(x), \quad f(x, 0) = \delta(x - x_0), \tag{1}$$

where $x_0 > 0$ is the initial point, K_α is the generalised diffusion coefficient and ${}_x D_\alpha^\beta$ for $0 < \alpha \leq 2$ is an asymmetric space-fractional derivative operator of order α and asymmetry parameter β , which is defined in the Fourier space as follows [72–75],

$$\mathcal{F} \left[{}_x D_\alpha^\beta f(x) \right] (k) = -\psi_\alpha^\beta(k) \mathcal{F} [f(x)](k), \tag{2}$$

where:

$$\psi_\alpha^\beta(k) = |k|^\alpha (1 - i\beta \operatorname{sgn} k \tan(\alpha\pi/2)), \quad 0 < \alpha \leq 2, \quad -1 \leq \beta \leq 1. \tag{3}$$

In this paper, we exclude the special case $\alpha = 1$ and $\beta \neq 0$ that requires special attention. For convenience, in the analytical point of view we use the characteristic function in the form:

$$\psi_\alpha^\rho(k) = (ik)^\alpha e^{-i\pi\alpha\rho \operatorname{sgn} k}, \quad 1 - \min(1, 1/\alpha) < \rho < \min(1, 1/\alpha), \tag{4}$$

where the following relation between the parameters is established (see details in Appendix A) [63,72]:

$$\rho = \frac{1}{2} + \frac{1}{\alpha\pi} \arctan(\beta \tan(\alpha\pi/2)). \tag{5}$$

Equation (1) is a generalisation of the space-fractional diffusion equation for symmetric Lévy flights [15] in the presence of a δ -sink of strength $\wp_{fa}(t)$ [53], and describes a target search by a walker exploring its accessible one-dimensional space by performing left-right asymmetrical random jumps represented by the asymmetric space-fractional derivative operator (2). The scale parameter K_α (along with the stable index α) physically sets the size

of the Lévy flight jumps. The skewness parameter β may be related to an effective drift or counter-gradient effect [76,77].

The consequence of the point sink at $x = 0$ is that the random walker is removed once the target is hit (see Figure 1). Thus, the time dependent weight $\wp_{fa}(t)$ is the first-arrival probability density. By integration of Equation (1) over the position co-ordinate x , we obtain that $\wp_{fa}(t)$ is the negative time derivative of the survival probability $\int_{-\infty}^{\infty} dx f(x, t)$ [53], i.e.,

$$\wp_{fa}(t) = -\frac{d}{dt} \int_{-\infty}^{\infty} dx f(x, t). \tag{6}$$

This means that $\wp_{fa}(t)$ is the probability density function (PDF) of first-arrival: once a random walker arrives at the sink it is annihilated. In what follows, we solve Equation (1) with the help of the Fourier–Laplace transform and various properties of the Mittag–Leffler and Fox H -functions (see Appendix B).

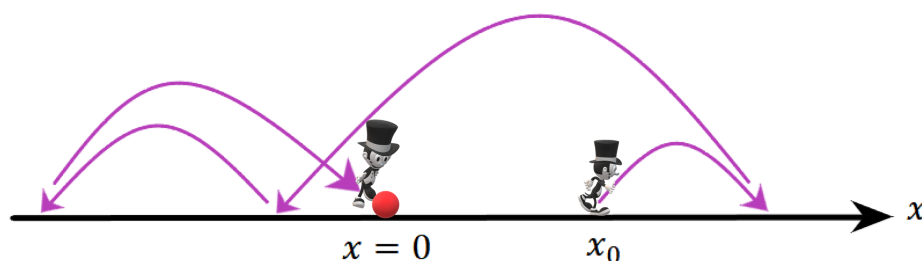


Figure 1. Schematic of the random search process. A walker starts its motion from x_0 and performs random jumps in the search space until he finds the target at $x = 0$.

2.1. Diffusion Equation for Asymmetric Lévy Flights

Application of the Fourier transform to Equation (1) yields:

$$\frac{\partial}{\partial t} f(k, t) = -\mathcal{D}_\alpha \psi_\alpha^\rho(k) f(k, t) - \wp_{fa}(t), \tag{7}$$

where [63,72]:

$$\mathcal{D}_\alpha = \frac{K_\alpha}{\cos(\alpha\pi(\rho - 1/2))}. \tag{8}$$

Let us first consider Equation (7) without the δ -sink, for the initial condition $f(x, 0) = \delta(x - x_0)$. In the Fourier–Laplace space, the solution is given by:

$$f(k, s) = \frac{\exp(ikx_0)}{s + \mathcal{D}_\alpha \psi_\alpha^\rho(k)}, \tag{9}$$

from which it follows that:

$$f(k, t) = \exp\left(-\mathcal{D}_\alpha \psi_\alpha^\rho(k)t + ikx_0\right). \tag{10}$$

Note that solution (10) can be easily obtained from Equation (7) without applying the Laplace transform. We add here Equation (9) in order to be consistent with the formula, including the sink, see Equation (14) below. Applying the inverse Fourier transform, we find (see details in Appendix C) [73]:

$$f(x, t) = \frac{1}{(\mathcal{D}_\alpha t)^{1/\alpha}} L_\alpha^\rho\left(\frac{x - x_0}{(\mathcal{D}_\alpha t)^{1/\alpha}}\right), \quad 0 < \alpha \leq 2, \tag{11}$$

where $L_\alpha^\rho(z)$ is the Lévy α -stable PDF defined as (A22) in terms of the H -function and $z > 0$. In Figure 2, we plot the PDF of Lévy flights with different stable index α and asymmetry parameter β . From Equation (11), by help of the Mellin transform of the H -function (A17) and the symmetry property $L_\alpha^\rho(-z) = L_\alpha^{1-\rho}(z)$ [72], we obtain the q th-order moment:

$$\langle |x|^q(t) \rangle = \frac{\sin(\pi\rho q) + \sin(\pi(1-\rho)q)}{\pi q} \Gamma(1+q)\Gamma(1-q/\alpha)(\mathcal{D}_\alpha t)^{q/\alpha}, \quad -1 < q < \alpha. \quad (12)$$

One can check that the moments in (12) are positive (see details in Appendix D). Note that for the case $0 < \alpha < 1$ with $\beta = -1, 1$, corresponding to $\rho = 0, 1$ respectively, the q th-order moment reads:

$$\langle |x|^q(t) \rangle = \frac{\Gamma(1-q/\alpha)}{\Gamma(1-q)} (\mathcal{D}_\alpha t)^{q/\alpha}, \quad -\infty < q < \alpha, \quad (13)$$

where we use Euler’s reflection formula. For the symmetric case ($\rho = 1/2$), we recover the result for symmetric Lévy flights [78–80].

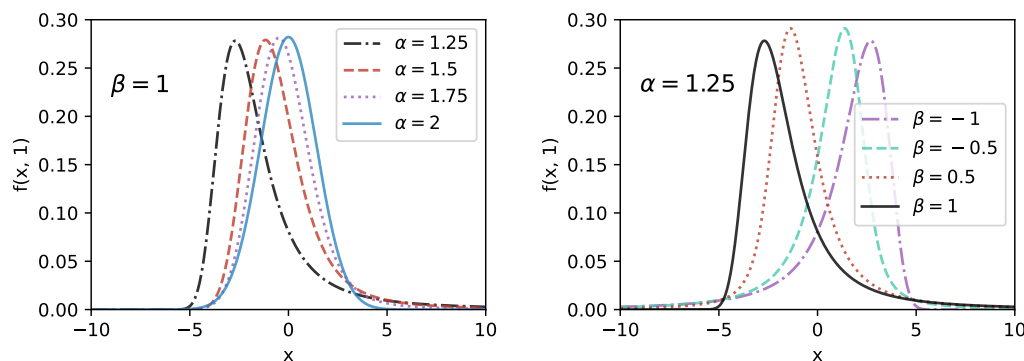


Figure 2. Probability density function of Lévy flights with $K_\alpha = 1$ at time $t = 1$. The value $\alpha = 2$ is the Gaussian limit, so that β become irrelevant and the PDF is symmetric.

2.2. Presence of the δ -Sink and Calculation of the First-Arrival Density

Let us now consider the model, including the δ -sink. The solution of Equation (1), for the initial condition $f(x, 0) = \delta(x - x_0)$, in Fourier–Laplace space is given by:

$$f(k, s) = \frac{\exp(ikx_0) - \wp_{fa}(s)}{s + \mathcal{D}_\alpha \psi_\alpha^\rho(k)}. \quad (14)$$

By integration of Equation (14) over k we find:

$$\int_{-\infty}^{\infty} dk f(k, s) = f(x = 0, s) = 0. \quad (15)$$

Thus, the first-arrival density in the Laplace domain reads:

$$\wp_{fa}(s) = \frac{I_2(s)}{I_1(s)}, \quad (16)$$

where for $I_1(s)$ and $I_2(s)$, we obtain (see details in Appendix E):

$$I_1(s) = \int_{-\infty}^{\infty} dk \frac{1}{s + \mathcal{D}_\alpha \psi_\alpha^\rho(k)} = \frac{2\pi s^{1/\alpha-1} \sin(\pi\rho)}{\alpha \mathcal{D}_\alpha^{1/\alpha} \sin(\pi/\alpha)}, \quad \alpha > 1 \quad (17)$$

and,

$$I_2(s) = \int_{-\infty}^{\infty} dk \frac{\exp(ikx_0)}{s + \mathcal{D}_\alpha \psi_\alpha^\rho(k)} = \frac{2\pi}{\alpha x_0} \frac{1}{s} H_{2,3}^{2,1} \left[\frac{x_0}{\mathcal{D}_\alpha^{1/\alpha}} s^{1/\alpha} \left| \begin{matrix} (1, 1/\alpha), (1, 1-\rho) \\ (1, 1/\alpha), (1, 1), (1, 1-\rho) \end{matrix} \right. \right]. \quad (18)$$

We mention that for $\alpha < 1$, $I_2(s)$ is finite while $I_1(s)$ diverges for any s , i.e., $\wp_{fa}(s) = 0$. For $\alpha = 1$, with $\beta = 0$ ($\rho = 1/2$), $I_2(s)$ is finite for $s \neq 0$, whereas $I_1(s)$ still diverges for $s > 0$, thus we have $\wp_{fa}(s) = 0$ again. In the case $\alpha > 1$ both $I_1(s)$ and $I_2(s)$ converge for finite s , thus, $\wp_{fa}(s)$ is non-zero [28,55]. Equation (16) then assumes the form:

$$\wp_{fa}(s) = \frac{\mathcal{D}_\alpha^{1/\alpha} \sin(\pi/\alpha)}{x_0 s^{1/\alpha} \sin(\pi\rho)} H_{2,3}^{2,1} \left[\frac{x_0}{\mathcal{D}_\alpha^{1/\alpha}} s^{1/\alpha} \middle| \begin{matrix} (1, 1/\alpha), (1, 1 - \rho) \\ (1, 1/\alpha), (1, 1), (1, 1 - \rho) \end{matrix} \right], \quad 1 < \alpha \leq 2. \quad (19)$$

By help of the inverse Laplace transform (see Equation (A16)) the first-arrival density yields as:

$$\wp_{fa}(t) = \frac{t^{-1+1/\alpha} \sin(\pi/\alpha)}{x_0 \mathcal{D}_\alpha^{-1/\alpha} \sin(\pi\rho)} H_{3,3}^{2,1} \left[\frac{x_0}{(\mathcal{D}_\alpha t)^{1/\alpha}} \middle| \begin{matrix} (1, 1/\alpha), (1, 1 - \rho), (1/\alpha, 1/\alpha) \\ (1, 1/\alpha), (1, 1), (1, 1 - \rho) \end{matrix} \right], \quad \alpha > 1. \quad (20)$$

Note that for $\alpha = 2$, i.e., $\rho = 1/2$, $\mathcal{D}_2 \equiv K_2$, by using the reduction property of the H -function (see relations (A13) and (A14)), we obtain the Lévy–Smirnov distribution:

$$\begin{aligned} \wp_{fa}(t) &= \frac{K_2^{1/2} t^{-1/2}}{x_0} H_{1,1}^{1,0} \left[\frac{x_0}{(K_2 t)^{1/2}} \middle| \begin{matrix} (1/2, 1/2) \\ (1, 1) \end{matrix} \right] = \frac{2x_0}{\sqrt{K_2 t^3}} H_{1,1}^{1,0} \left[\frac{x_0^2}{K_2 t} \middle| \begin{matrix} (-1/2, 1) \\ (-1, 2) \end{matrix} \right] \\ &= \frac{x_0}{\sqrt{4\pi K_2 t^3}} H_{0,1}^{1,0} \left[\frac{x_0^2}{4K_2 t} \middle| \begin{matrix} (0, 1) \end{matrix} \right] = \frac{x_0}{\sqrt{4\pi K_2 t^3}} \exp\left(-\frac{x_0^2}{4K_2 t}\right). \end{aligned} \quad (21)$$

In the latter equality, we used Equation (A10) and the duplication rule $2^{2z}\Gamma(z)\Gamma(z + 1/2) = 2\sqrt{\pi}\Gamma(2z)$ of the Γ -function. By help of Equations (A11) and (A12) the first-arrival density (20) can be expressed in the following form:

$$\wp_{fa}(t) = \frac{t^{-1+1/\alpha} \alpha \sin(\pi/\alpha)}{x_0 \mathcal{D}_\alpha^{-1/\alpha} \sin(\pi\rho)} H_{3,3}^{1,2} \left[\frac{\mathcal{D}_\alpha t}{x_0^\alpha} \middle| \begin{matrix} (0, 1), (0, \alpha), (0, \alpha - \alpha\rho) \\ (0, 1), (0, \alpha - \alpha\rho), (1 - 1/\alpha, 1) \end{matrix} \right]. \quad (22)$$

Inserting the series expansion of the H -function (A8) we obtain:

$$\begin{aligned} \wp_{fa}(t) &= \frac{t^{-1+1/\alpha} \alpha \sin(\pi/\alpha)}{x_0 \mathcal{D}_\alpha^{-1/\alpha} \sin(\pi\rho)} \sum_{k=1}^{\infty} \frac{\Gamma(1+k)\Gamma(1+\alpha k)}{\Gamma(1+\alpha k - \alpha\rho k)\Gamma(1/\alpha + k)\Gamma(\alpha\rho k - \alpha k)} \frac{(-1)^k}{k!} \left(\frac{\mathcal{D}_\alpha t}{x_0^\alpha}\right)^k \\ &= \frac{t^{-1+1/\alpha} \alpha \sin(\pi/\alpha)}{x_0 \mathcal{D}_\alpha^{-1/\alpha} \pi \sin(\pi\rho)} \sum_{k=1}^{\infty} (-1)^{k-1} \sin(\pi\alpha(1 - \rho)k) \frac{\Gamma(1 + \alpha k)}{\Gamma(1/\alpha + k)} \left(\frac{\mathcal{D}_\alpha t}{x_0^\alpha}\right)^k. \end{aligned} \quad (23)$$

This form can be shown to be equivalent to the corresponding expression in Theorem 3.14 of [52], in a dimensionless form. Therefore, from the equation above, the short time limit of the first-arrival density has the asymptotic behaviour

$$\wp_{fa}(t) \sim \frac{\alpha \sin(\pi/\alpha) \sin(\pi\alpha(1 - \rho))}{\pi \sin(\pi\rho)} \frac{\Gamma(1 + \alpha)}{\Gamma(1/\alpha + 1)} \frac{\mathcal{D}_\alpha^{1+1/\alpha}}{x_0^{1+\alpha}} t^{1/\alpha}. \quad (24)$$

We also provide another method to get the above expression in Appendix F.

In order to obtain the long time limit, we use the Laplace transform of the first-arrival density (19) at small s , and then apply the Tauberian theorem [81] to get (see Appendix F for details):

$$\wp_{fa}(t) \sim \frac{\sin(\pi\alpha(1 - \rho))}{\sin(\pi\rho)} \frac{\Gamma(2 - \alpha)}{\Gamma^2(1/\alpha)\Gamma(1 - 1/\alpha)} \frac{\mathcal{D}_\alpha^{-1+1/\alpha}}{x_0^{1-\alpha}} t^{-2+1/\alpha}. \quad (25)$$

This expression is in agreement with the results in [53] for the symmetric case ($\beta = 0$). Note that the short and long time limit behaviours are also in agreement with intuition, namely, the first-arrival density initially increases from zero as a power of time t , and asymptotically decreases with a negative power of t (we note that this derivation assumed

$\alpha > 1$). Note also that, with the variation of ρ (see Equation (5)), Equations (24) and (25) are non-negative.

The fractional-order moments of the first-arrival density with $1 < \alpha < 2$ read:

$$\langle t^q \rangle = \int_0^\infty dt t^q \wp_{fa}(t) = \frac{\sin(\pi/\alpha) \sin(\pi(1-\rho)(1+\alpha q)) \Gamma(1-\alpha q) x_0^{\alpha q}}{\sin(\pi\rho) \sin(\frac{\pi}{\alpha}(1+\alpha q)) \Gamma(1-q) \mathcal{D}_\alpha^q},$$

$$-1 - \frac{1}{\alpha} < q < 1 - \frac{1}{\alpha}, \quad \beta \neq 1, \tag{26}$$

where we use the Mellin transform of the H -function (see Equation (A17)). This form can be shown to be equivalent to the corresponding result in [52] (see Theorem 3.9). Due to the definition of ρ (Equation (5)), and from variations of q , it is obvious that the moments are positive. For the case $\beta = 1$ with $1 < \alpha < 2$, we have $\rho = 1 - 1/\alpha$, and thus arrive at:

$$\langle t^q \rangle = \frac{\Gamma(1-\alpha q) x_0^{\alpha q}}{\Gamma(1-q) \mathcal{D}_\alpha^q}, \quad -\infty < q < \frac{1}{\alpha}, \quad \beta = 1, \tag{27}$$

while for the limit of Brownian motion ($\alpha = 2$), we get:

$$\langle t^q \rangle = \frac{\Gamma(1-2q) x_0^{2q}}{\Gamma(1-q) K_2^q}, \quad -\infty < q < \frac{1}{2}. \tag{28}$$

In Figure 3, we plot the fractional-order moments of symmetric ($\beta = 0$) and the extremal two-sided ($\beta = 1$) Lévy flights as functions of the parameter q for different values of the stable index α . As can be seen, the PDFs are normalised, $\langle t^{q=0} \rangle = 1$, but have diverging means for all α .

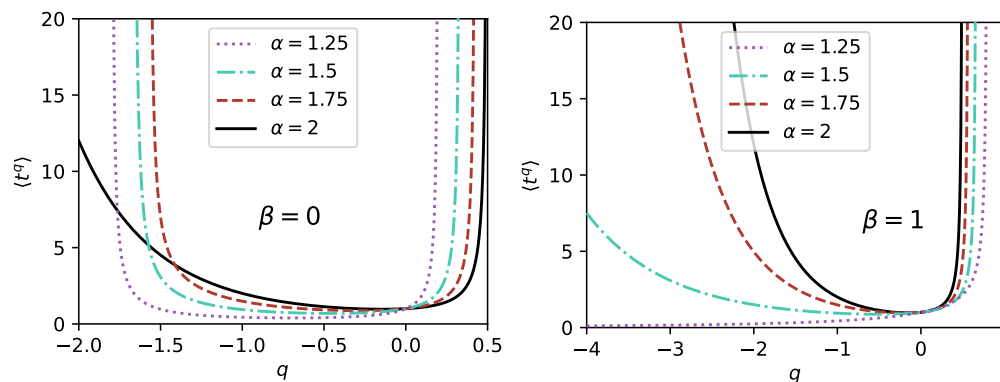


Figure 3. Fractional-order moments of the first-arrival density of Lévy flights for $x_0 = 1$ and $K_\alpha = 1$.

3. Langevin Equation Approach

A complementary view to the calculation of time dependent probabilities is the numerical study of individual search paths. For such a simulation of asymmetric Lévy flights, we use the (stochastic) Langevin equation for the particle position x [67],

$$\frac{dx(t)}{dt} = K_\alpha^{1/\alpha} \zeta(t), \tag{29}$$

driven by random noise $\zeta(t)$ with Lévy stable distribution, which is characterised by the stable index α and the asymmetry parameter β . For simulation purposes we pass to the discretised version of the Langevin equation,

$$x_{n+1} - x_n = (K_\alpha \Delta t)^{1/\alpha} \zeta_t, \tag{30}$$

taken at times $t_n = n\Delta t$, $n = 0, 1, 2, \dots$, for more details, see [67]. The noise ζ_t is computed according to the algorithm described in [82]. For each fixed value of α , β and K_α , the random walker starts its motion at x_0 . When it hits the vicinity of the origin $x = 0$, the corresponding event time $t = n\Delta t$ is recorded and a new particle is released. This procedure is repeated 2×10^6 times. The time steps to determine the long-time and short-time behaviours of the first-arrival density were $\Delta t = 0.001$ and 0.0001 , respectively. For the very short-time behaviour when $t \rightarrow 0$ we chose $\Delta t = 0.00001$. While we study analytically a point-like target, in the simulations, we have to endow the target with a finite size d . This size should be sufficiently large to be detected by the simulated walk—and small enough to be considered as a point-like target and thus warrant proper statistics. This issue was discussed in detail in [9,54]. We find that the appropriate size of the target should be $d \sim 2(\mathcal{D}_\alpha \Delta t)^{1/\alpha}$, as a function of the time step Δt , stable index α , asymmetry parameter β and the generalised diffusion coefficient K_α (see Equations (5) and (8)). Note that in contrast to the symmetric case $\beta = 0$ studied in [9,54], here, the coefficient \mathcal{D}_α depends on both α and β , such that we should choose a smaller time step for simulations with α closer to unity.

Figure 4 shows the long-time asymptotic behaviour of the first-arrival PDF along with the short-time behaviour and the behaviour around $t = 0$, respectively. The coloured solid curves in the left and centre panels are obtained from the exact analytical solution (20), and the symbols show the results based on numerical solution of the Langevin Equation (30). The short black lines in the right panels represent the long-time asymptotic behaviour $t^{-2+1/\alpha}$ (see Equation (25)). From the short-time behaviour of the first-arrival density in Figure 4 (left and centre panels), it can be seen that, initially (at $t \leq 0.1$), particles moving with negative skewness ($\beta < 0$) have a higher chance to find the target as compared with particles with non-negative β . In physical terms, the negative skewness corresponds to shorter jumps to the right occurring with higher frequency and longer jumps occurring with lower frequency to the left. However, it is seen from the centre panels that at times longer than 0.1 the random walker with positive β will detect the target with higher probability. This is intuitively clear since such a walker performs more short jumps to the negative direction (towards the target) for positive β , and when α tends to 1^+ the number of short jumps increases. Thus, the area on the left of the initial position x_0 is densely covered, whereas the random searcher with $\beta < 0$ performs long jumps to the left direction and may more easily overshoot the target.

The short-time behaviour of the first-arrival density of asymmetric Lévy flights is depicted in Figure 5 for different values of the stable index α and diffusion coefficient $K_\alpha = 10$. The results obtained from simulations (coloured symbols) are in good agreement with the theoretical result (20). One can see that for the case $\beta = 1$ (left panel), the searcher with smaller stable index α will find the target faster since, in this case, there are more short jumps in the direction of the target. Respectively, in case of the negative skewness $\beta = -0.5$ (right panel) the searcher with larger α will find the target faster. These observations—valid for close initial distance between the searcher and the target ($x_0 = 1$)—are confirmed by calculation of the search efficiency in the next Section. We note that, based on the simulations whose results are shown in Figures 4 and 5 for different time scales, the first-arrival probability densities are unimodal.

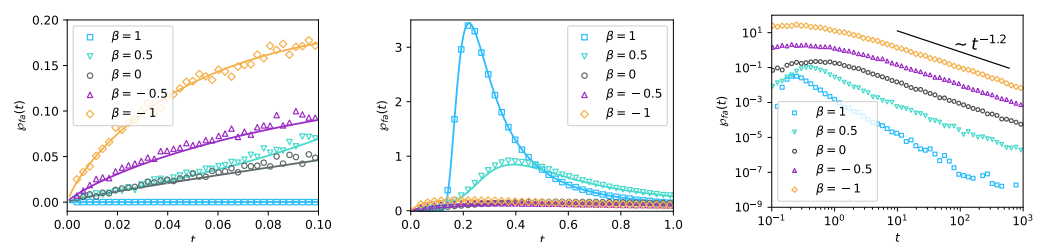


Figure 4. Cont.

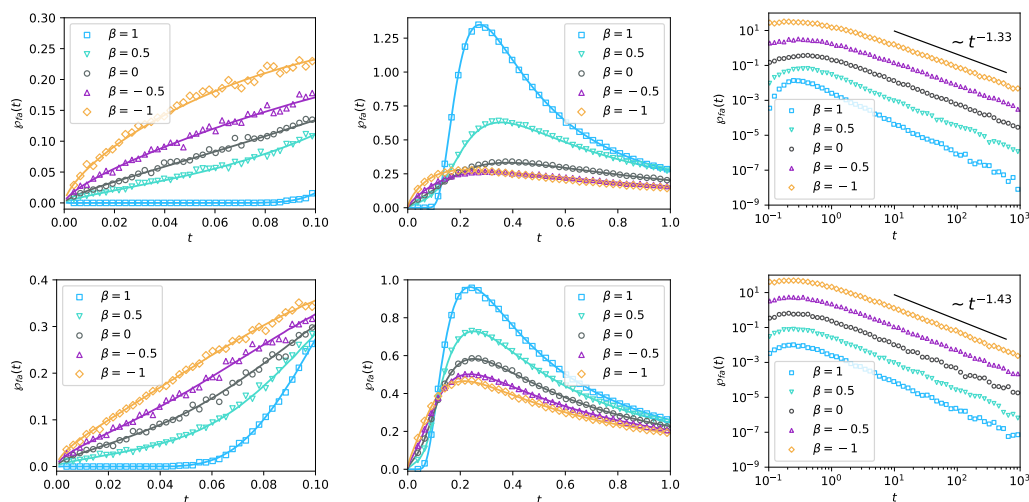


Figure 4. Left and centre: short-time behaviour for the first-arrival density of Lévy flights with different β , for $\alpha = 1.25, 1.5$ and 1.75 , from top to bottom, respectively. The solid lines are computed from the full expression (20). The coloured symbols depict the simulation results of the Langevin Equation (29). Right: same as the left panels but depicting the long-time behaviour. The short black line shows the asymptote $t^{-2+1/\alpha}$. Note that for better visual comparison the results are multiplied by a factor of 0.01 for $\beta = 1$, of 0.1 for $\beta = 0.5$, of 10 for $\beta = -0.5$ and of 100 for $\beta = -1$. We chose the time steps $\Delta t = 0.00001$ for the $t \rightarrow 0$ limit in the left panels, $\Delta t = 0.0001$ to simulate the short-time behaviour in the middle panels and $\Delta t = 0.001$ for the long-time behaviour in the right panels, with $N = 2 \times 10^6$ realisations. Moreover, $K_\alpha = 1$ and with $x_0 = 1$, and the target size was chosen as $2(\mathcal{D}_\alpha \Delta t)^{1/\alpha}$. We note that for the case $\beta = 1$, a decrease of α means that the long-time asymptotic behaviour will be observed at longer times.

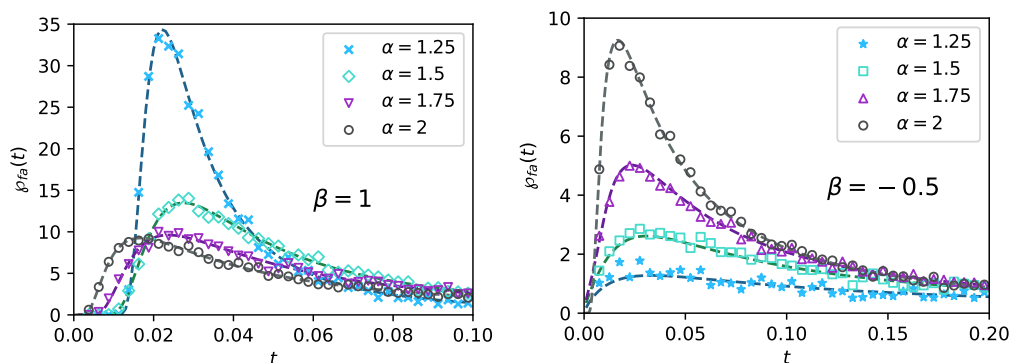


Figure 5. Short-time asymptotic of the first-arrival density of Lévy flights for different stable index α with $K_\alpha = 10$ and $x_0 = 1$. Symbols show the simulation results based on the Langevin approach and the dashed lines are computed from the exact analytical expression (20). We chose $\Delta t = 0.0001$ for $N = 2 \times 10^6$ realisations, and the target size is $2(\mathcal{D}_\alpha \Delta t)^{1/\alpha}$.

4. Calculation of the Search Efficiency

In order to study the search efficiency, we make use of the definition proposed in [9], which is defined by:

$$\mathcal{E} = \left\langle \frac{1}{t} \right\rangle = \int_0^\infty dt \frac{\wp_{fa}(t)}{t} = \int_0^\infty ds \wp_{fa}(s). \tag{31}$$

A given search strategy is optimal when the efficiency \mathcal{E} of the corresponding search process reaches its maximum. The constructive meaning of such a definition of efficiency was tested in [9] for Brownian motion with drift towards and away from the target. The expediency of the definition was addressed in the first arrival problems for symmetric Lévy

flights with drift in [9], for combined Lévy–Brownian and Lévy–Lévy search in [55,83] of single and multiple targets. In all the cases, such a definition gives reasonable results, which allow explanation at an intuitive level. Another strong motivation is its analytical simplicity, which allows for getting exact analytical formulas in cases where the most probable value of the first arrival time can be calculated only numerically.

The exact result for the search efficiency can be obtained by substituting Equation (19) or (20) into the above expression and then using equation (A17). We find that:

$$\mathcal{E} = \frac{\sin[\pi(1-\rho)(\alpha-1)]}{\sin(\pi\rho)} \Gamma(\alpha+1) \frac{\mathcal{D}_\alpha}{x_0^\alpha}. \quad (32)$$

Consequently, in general, the efficiency depends on the positive parameter ρ and, hence, on the skewness parameter β . In particular, for the symmetric case $\rho = 1/2$ or $\beta = 0$ it turns out that [9]:

$$\mathcal{E} = \sin\left(\frac{\pi}{2}(\alpha-1)\right) \Gamma(\alpha+1) \frac{\mathcal{D}_\alpha}{x_0^\alpha}, \quad (33)$$

and in the limit $\alpha = 2$ for a Brownian walker, the efficiency is given by:

$$\mathcal{E} = \frac{2\mathcal{D}_2}{x_0^2}. \quad (34)$$

In the Cauchy limit $\alpha = 1$ ($\beta = 0$), the efficiency goes to zero. For the case $\alpha \rightarrow 1^+$ with $\beta \neq 0$, substituting Equations (5) and (8) into Equation (32) yields:

$$\mathcal{E} = \frac{\sin\left[\left(\frac{\pi}{2} - \frac{1}{\alpha} \arctan\left(\beta \tan\left(\frac{\alpha\pi}{2}\right)\right)\right)(\alpha-1)\right]}{\cos\left[\frac{1}{\alpha} \arctan\left(\beta \tan\left(\frac{\alpha\pi}{2}\right)\right)\right] \cos\left[\arctan\left(\beta \tan\left(\frac{\alpha\pi}{2}\right)\right)\right]} \frac{\Gamma(\alpha+1)K_\alpha}{x_0^\alpha}. \quad (35)$$

Finally, taking the limit $\alpha \rightarrow 1^+$, one gets (see details in Appendix G):

$$\mathcal{E} = \begin{cases} \infty & \beta > 0 \\ \frac{2|\beta|}{\pi} \frac{K_\alpha}{x_0} & \beta < 0 \end{cases}. \quad (36)$$

In Figures 6–8, we use Equation (32) to compare the search efficiency for different values of the stable index α , skewness β and initial distance x_0 . In Figure 6, we show the dependence of the search efficiency on the stable index α for different values of β . We observe that when the target is located on the left of the random searcher at the initial distance x_0 , it is more probable to be detected by Brownian motion than by Lévy flights with non-positive asymmetry parameter ($\beta \leq 0$). This is intuitively clear: in contrast to the Brownian walker, such a Lévy searcher performs long jumps to the left, which may easily lead him far away from the target located at $x = 0$. Vice versa, Lévy flights with $\beta > 0$ are always more efficient than Brownian search since for such searchers long jumps to the left are forbidden, while they perform more shorter jumps to the left than the Brownian walker. Such an intuitive picture stems from the shapes of the α -stable PDFs depicted in the left panel of Figure 2.

In Figure 7, we illustrate the dependency of the search efficiency on the asymmetry parameter β for different stable index α and for two different initial target distances. It can be seen that for the close target ($x_0 = 0.5$) Brownian motion is more efficient than the Lévy search (except for Lévy flights with $\beta > 0$ and $\alpha \rightarrow 1$). By increasing the initial distance, Lévy flights are more efficient as compared to the Brownian motion (except for $\alpha = 1$ with $\beta = 0$). Moreover, the asymmetry in the jumps leads to a higher efficiency, and this effect is more pronounced for stable indices close to unity.

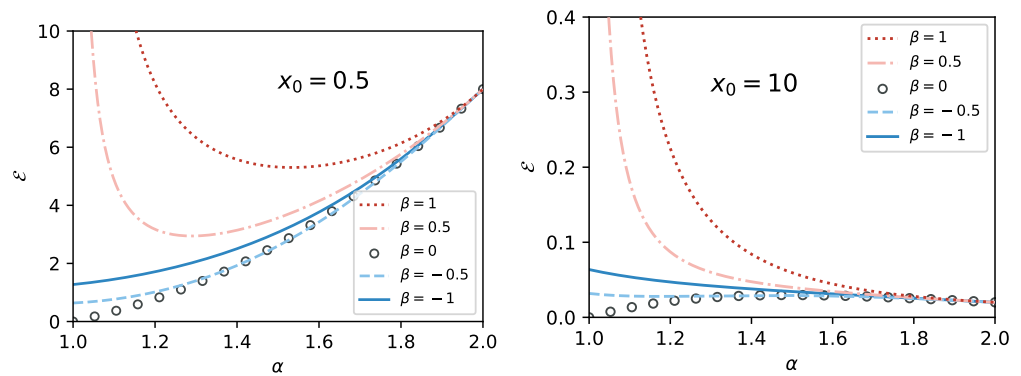


Figure 6. Search efficiency \mathcal{E} as function of the stable index α for different values of the skewness parameter β with $K_\alpha = 1$.

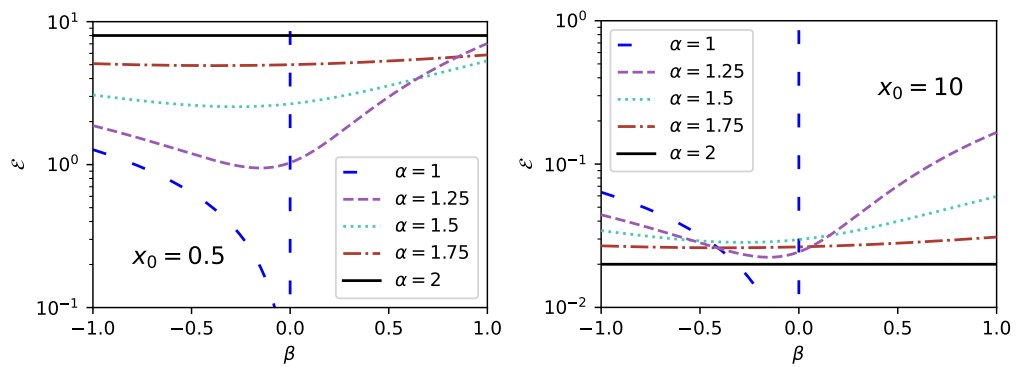


Figure 7. Search efficiency \mathcal{E} as function of the skewness parameter β for different values of α with $K_\alpha = 1$ in log-linear scale.

Finally, we study the effect of the initial distance x_0 on the search efficiency for different values of the asymmetry β in Figure 8. It was observed that for smaller values of α , the asymmetry of the jumps led to higher search efficiency, and by increasing $\alpha \rightarrow 2$ at a fixed value of x_0 , all Lévy flights have almost the same search efficiency.

Another important quantity is the search reliability, defined as the cumulative arrival probability [9],

$$\mathcal{P} = \int_0^\infty dt \varphi_{fa}(t). \tag{37}$$

From relation (20), we find that $\mathcal{P} = 1$, which means that in the case of asymmetric Lévy flights, as in the case of symmetric Lévy flights, the searcher will always find the target, and this statement is valid for $\alpha > 1$ with all β ($-1 \leq \beta \leq 1$).

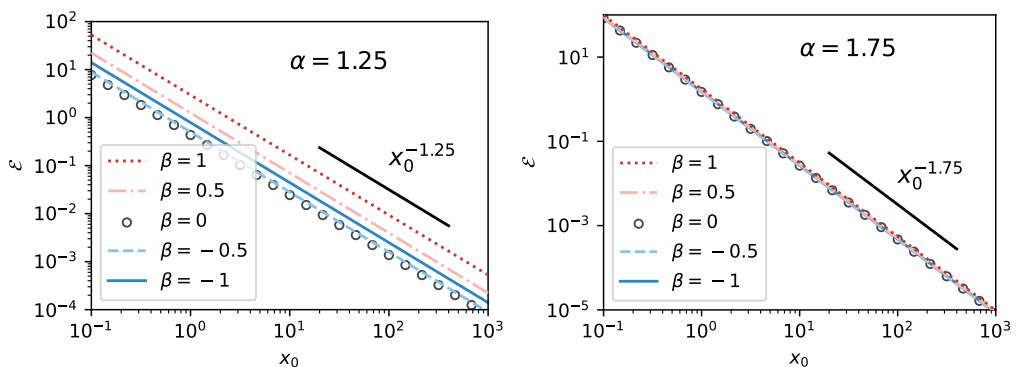


Figure 8. Search efficiency \mathcal{E} as function of the initial position x_0 for different β with $K_\alpha = 1$ on log-log scale. The short solid line shows the asymptote $x_0^{-\alpha}$ (see Equation (32)).

5. Conclusions

We investigated the dynamics and performance of asymmetric Lévy flights as a random search strategy by solving the deterministic Fokker–Planck equation with asymmetric space-fractional derivative in the presence of a sink, which mimics a point target. We found exact results for the resulting first-arrival or first-hitting density, its fractional order moments and search efficiency in terms of the stable index α and the skewness parameter β of the asymmetric Lévy flight. We observed that the first-arrival density is identically zero for processes with $\alpha \leq 1$. For $\alpha > 1$ the first-arrival density increases at short times as $t^{1/\alpha}$ and decreases at long times as $t^{-2+1/\alpha}$. Thus, the exponents of the short- and long-time asymptotics are independent of the skewness β .

The efficiency of the search depends on both parameters, the stable index and skewness, as well as on the initial distance x_0 of the searcher to the target and the diffusion coefficient K_α . We demonstrated that for a short initial distance x_0 , the Brownian strategy is more efficient than Lévy flights, except when $\beta > 0$ with stable index $\alpha \rightarrow 1$. For long initial distances, Lévy flights become more efficient than the Brownian motion. These observations extend the results obtained in [9] to the asymmetric case. We also found that the asymmetry in jump yields higher efficiency, especially for stable indices close to unity. In the limiting case $\alpha \rightarrow 1^+$, the search efficiency is infinite for positive skewness, and the situation drastically changes for a negative skewness. It is observed that the search efficiency in this limit case has a linear behaviour with respect to $|\beta|$.

It will be interesting to analyse the case of asymmetric Lévy flight search on multiple targets, as was done for symmetric Lévy flights [83]. Another interesting search strategy could be the case of combined search [55]: asymmetric Lévy flights with local Brownian search. It is also of interest to study the random Lévy search in two and three dimensions, as well as applications of such non-local asymmetric search processes in finding the global extremum of potential functions [59]. Different definitions of the search efficiency are also worth being analysed and compared.

Author Contributions: Conceptualisation, T.S., R.M. and A.V.C.; methodology, A.P., T.S., H.K., R.M. and A.V.C.; software, A.P.; formal analysis, A.P.; investigation, A.P., T.S. and A.V.C.; writing—original draft preparation, A.P., T.S., H.K., R.M. and A.V.C.; writing—review and editing, A.P., T.S., H.K., R.M. and A.V.C.; visualisation, A.P.; supervision, H.K., R.M. and A.V.C. All authors contributed to each part of this work equally. All authors have read and agreed to the published version of the manuscript.

Funding: T.S. was supported by the Alexander von Humboldt Foundation. T.S. also acknowledges support from the bilateral Macedonian-Chinese research project 20-6333, funded under the inter-governmental Macedonian-Chinese agreement. T.S. and R.M. acknowledge financial support by the German Science Foundation (DFG, Grant number ME 1535/12-1). R.M. acknowledges support from the Foundation for Polish Science (Fundacja na rzecz Nauki Polskiej, FNR) within an Alexander von Humboldt Honorary Polish Research Scholarship. A.V.C. acknowledges support of the Polish National Agency for Academic Exchange (NAWA).

Conflicts of Interest: The authors declare no conflict of interest.

Abbreviations

The following abbreviation is used in this manuscript:

PDF Probability density function

Appendix A. Characteristic Functions of α -Stable Processes

Among different forms for the parametrisation of α -stable laws in the literature, where each form might be useful in a particular situation, we here present the standard form of the characteristic function and show how to derive the Z-form [63,72] which is used in the main text as more convenient for our purposes in analytical calculations. The standard form of the characteristic function reads [84]:

$$f(k, t) = e^{-K_\alpha \psi_\alpha^\beta(k)t} = \exp(-K_\alpha t |k|^\alpha [1 - i\beta \tan(\alpha\pi/2) \operatorname{sgn}k]), \quad 0 < \alpha \leq 2, \quad -1 \leq \beta \leq 1. \tag{A1}$$

We exclude the case $\alpha = 1$ and $\beta \neq 0$. Changing the variable $\beta \tan(\alpha\pi/2) = \tan(\beta' \mathcal{K}(\alpha)\pi/2)$ leads to:

$$\begin{aligned} f(k, t) &= \exp\left(-K_\alpha t |k|^\alpha \left[1 - i \tan\left(\beta' \mathcal{K}(\alpha)\pi/2\right) \operatorname{sgn}k\right]\right) \\ &= \exp\left(-\frac{K_\alpha t}{\cos(\beta' \mathcal{K}(\alpha)\pi/2)} |k|^\alpha \left[\cos(\beta' \mathcal{K}(\alpha)\pi/2) - i \sin(\beta' \mathcal{K}(\alpha)\pi/2) \operatorname{sgn}k\right]\right) \\ &= \exp\left(-\frac{K_\alpha t}{\cos(\beta' \mathcal{K}(\alpha)\pi/2)} |k|^\alpha \exp\left[-\frac{i\pi}{2} \beta' \mathcal{K}(\alpha) \operatorname{sgn}k\right]\right), \end{aligned} \tag{A2}$$

where $\mathcal{K}(\alpha) = \alpha - 1 + \operatorname{sgn}(1 - \alpha)$ [72]. Defining $\beta' \mathcal{K}(\alpha) = \alpha(2\rho - 1)$, leads us to the desired result:

$$f(k, t) = e^{-\mathcal{D}_\alpha \psi_\alpha^\rho(k)t} = \exp(-\mathcal{D}_\alpha t (ik)^\alpha \exp[-i\pi\alpha\rho \operatorname{sgn}k]), \tag{A3}$$

where:

$$\rho = \frac{1}{2} + \frac{1}{2\alpha} \beta' \mathcal{K}(\alpha) = \frac{1}{2} + \frac{1}{\alpha\pi} \arctan(\beta \tan(\alpha\pi/2)), \quad \mathcal{D}_\alpha = \frac{K_\alpha}{\cos(\alpha\pi(\rho - 1/2))}. \tag{A4}$$

Appendix B. Mittag–Leffler and Fox H -Functions

The two-parameter Mittag–Leffler (M-L) function has the series representation [85]:

$$E_{\alpha,\beta}(z) = \sum_{k=0}^{\infty} \frac{1}{\Gamma(\alpha k + \beta)} \frac{z^k}{k!}, \tag{A5}$$

and in the form of a Mellin–Barnes integral reads [86]:

$$E_{\alpha,\beta}(-z) = \frac{1}{2\pi i} \int_{\Omega} ds \frac{\Gamma(-s)\Gamma(1+s)}{\Gamma(\beta + \alpha s)} z^s. \tag{A6}$$

The Fox H -function (or simply H -function) is defined by the following Mellin–Barnes integral [86]:

$$H_{p,q}^{m,n} \left[z \left| \begin{matrix} (a_1, A_1), \dots, (a_p, A_p) \\ (b_1, B_1), \dots, (b_q, B_q) \end{matrix} \right. \right] = H_{p,q}^{m,n} \left[z \left| \begin{matrix} (a_p, A_p) \\ (b_q, B_q) \end{matrix} \right. \right] = \frac{1}{2\pi i} \int_{\Omega} ds \Theta(s) z^s, \tag{A7}$$

where $\Theta(s) = \frac{\prod_{j=1}^m \Gamma(b_j - B_j s) \prod_{j=1}^n \Gamma(1 - a_j + A_j s)}{\prod_{j=m+1}^q \Gamma(1 - b_j + B_j s) \prod_{j=n+1}^p \Gamma(a_j - A_j s)}$, $0 \leq n \leq p$, $1 \leq m \leq q$, $a_i, b_j \in \mathbb{C}$, $A_i, B_j \in \mathbb{R}^+$, $i = 1, \dots, p$, $j = 1, \dots, q$. The contour Ω starting at $c - i\infty$ and ending at $c + i\infty$ separates the poles of the function $\Gamma(b_j - B_j s)$, $j = 1, \dots, m$ from those of the function $\Gamma(1 - a_i + A_i s)$, $i = 1, \dots, n$. The series expansion of the H -function is given by [86]:

$$\begin{aligned} &H_{p,q}^{m,n} \left[z \left| \begin{matrix} (a_p, A_p) \\ (b_q, B_q) \end{matrix} \right. \right] \\ &= \sum_{h=1}^m \sum_{k=0}^{\infty} \frac{\prod_{j=1, j \neq h}^m \Gamma\left(b_j - B_j \frac{b_h + k}{B_h}\right) \prod_{j=1}^n \Gamma\left(1 - a_j + A_j \frac{b_h + k}{B_h}\right)}{\prod_{j=m+1}^q \Gamma\left(1 - b_j + B_j \frac{b_h + k}{B_h}\right) \prod_{j=n+1}^p \Gamma\left(a_j - A_j \frac{b_h + k}{B_h}\right)} \frac{(-1)^k z^{(b_h + k)/B_h}}{k! B_h}. \end{aligned} \tag{A8}$$

The connection between the two parameter M-L function and Fox H -function is given by [86]:

$$E_{\alpha,\beta}(-z) = H_{1,2}^{1,1} \left[z \left| \begin{matrix} (0, 1) \\ (0, 1), (1 - \beta, \alpha) \end{matrix} \right. \right]. \tag{A9}$$

The relation between the exponential function and the Fox H -function reads:

$$B^{-1} z^{\frac{b}{B}} \exp\left(-z^{\frac{1}{B}}\right) = H_{0,1}^{1,0} \left[z \left| \frac{\quad}{(b, B)} \right. \right]. \tag{A10}$$

Moreover, the H -function has the following properties ($n \geq 1, q > m$):

$$H_{p,q}^{m,n} \left[z \left| \begin{matrix} (a_p, A_p) \\ (b_q, B_q) \end{matrix} \right. \right] = H_{q,p}^{n,m} \left[\frac{1}{z} \left| \begin{matrix} (1 - b_q, B_q) \\ (1 - a_p, A_p) \end{matrix} \right. \right], \tag{A11}$$

$$H_{p,q}^{m,n} \left[z \left| \begin{matrix} (a_p, A_p) \\ (b_q, B_q) \end{matrix} \right. \right] = c H_{p,q}^{m,n} \left[z^c \left| \begin{matrix} (a_p, cA_p) \\ (b_q, cB_q) \end{matrix} \right. \right], \quad c > 0, \tag{A12}$$

$$H_{p,q}^{m,n} \left[z \left| \begin{matrix} (a_j, A_j)_{1,p} \\ (b_j, B_j)_{1,q-1}, (a_1, A_1) \end{matrix} \right. \right] = H_{p-1,q-1}^{m,n-1} \left[z \left| \begin{matrix} (a_j, A_j)_{2,p} \\ (b_j, B_j)_{1,q-1} \end{matrix} \right. \right], \tag{A13}$$

$$H_{p,q}^{m,n} \left[z \left| \begin{matrix} (a_j, A_j)_{1,p-1}, (b_1, B_1) \\ (b_j, B_j)_{1,q} \end{matrix} \right. \right] = H_{p-1,q-1}^{m-1,n} \left[z \left| \begin{matrix} (a_j, A_j)_{1,p-1} \\ (b_j, B_j)_{2,q} \end{matrix} \right. \right]. \tag{A14}$$

The Laplace transform formula for the H -function is [86]:

$$\int_0^\infty dt e^{-st} t^\delta H_{p,q}^{m,n} \left[at^\sigma \left| \begin{matrix} (a_p, A_p) \\ (b_q, B_q) \end{matrix} \right. \right] = s^{-1-\delta} H_{p+1,q}^{m,n+1} \left[as^{-\sigma} \left| \begin{matrix} (-\delta, \sigma), (a_p, A_p) \\ (b_q, B_q) \end{matrix} \right. \right], \tag{A15}$$

where $\text{Re}(\delta + \sigma \min_{1 \leq j \leq m} (\frac{b_j}{B_j})) > -1, \delta \in \mathbb{C}, s \in \mathbb{C} (\text{Re}(s) > 0)$ and a, σ and θ are positive. The parameter θ defined by $\theta = \sum_{j=1}^n A_j - \sum_{j=n+1}^p A_j + \sum_{j=1}^m B_j - \sum_{j=m+1}^q B_j$. Moreover, the inverse Laplace transform of the H -function reads:

$$\mathcal{L}^{-1} \left\{ s^{-\delta} H_{p,q}^{m,n} \left[as^\sigma \left| \begin{matrix} (a_p, A_p) \\ (b_q, B_q) \end{matrix} \right. \right]; t \right\} = t^{\delta-1} H_{p+1,q}^{m,n} \left[at^{-\sigma} \left| \begin{matrix} (a_p, A_p), (\delta, \sigma) \\ (b_q, B_q) \end{matrix} \right. \right], \tag{A16}$$

where $\text{Re}(\delta + \sigma \max_{1 \leq i \leq n} (\frac{1}{A_i} - \frac{a_i}{A_i})) > 0, \delta, a, s \in \mathbb{C} (\text{Re}(s) > 0), |\arg a| < \frac{1}{2} \pi (\theta - \sigma)$ and $\sigma > 0$. The Mellin transform of the H -function is given by [86]:

$$\int_0^\infty dx x^\xi H_{p,q}^{m,n} \left[ax \left| \begin{matrix} (a_p, A_p) \\ (b_q, B_q) \end{matrix} \right. \right] = a^{-\xi} \Theta(-\xi), \tag{A17}$$

where $\Theta(\xi)$ is defined in Equation (A7).

Appendix C. Derivation of the Lévy α -Stable PDF

In order to obtain the solution of Equation (10), we first apply the inverse Fourier transform, namely,

$$\begin{aligned} \frac{1}{2\pi} \int_{-\infty}^\infty dk e^{-ikx} f(k, t) &= \frac{1}{2\pi} \int_{-\infty}^\infty dk e^{-ikx} \exp\left(-\mathcal{D}_\alpha \psi_\alpha^\rho(k) t + ikx_0\right) \\ &= \frac{1}{2\pi} \int_{-\infty}^\infty dk e^{-ikz} \exp\left(-\mathcal{D}_\alpha \psi_\alpha^\rho(k) t\right), \end{aligned} \tag{A18}$$

where $z = x - x_0$. By help of relation (A10) and using the Mellin–Barnes integral representation of the Fox H -function, we get:

$$\begin{aligned} \frac{1}{2\pi} \int_{-\infty}^{\infty} dk e^{-ikz} \exp\left(-\mathcal{D}_\alpha \psi_\alpha^\rho(k)t\right) &= \frac{1}{2\pi} \int_{-\infty}^{\infty} dk e^{-ikz} H_{0,1}^{1,0} \left[\mathcal{D}_\alpha \psi_\alpha^\rho(k)t \mid \frac{\quad}{(0,1)} \right] \\ &= \frac{1}{2\pi} \int_{-\infty}^{\infty} dk e^{-ikz} \frac{1}{2\pi i} \int_{\Omega} ds \Gamma(-s) \left(\mathcal{D}_\alpha \psi_\alpha^\rho(k)t\right)^s \\ &= \frac{1}{2\pi i} \int_{\Omega} ds \Gamma(-s) \frac{1}{2\pi} \int_{-\infty}^{\infty} dk e^{-ikz} \left(\mathcal{D}_\alpha \psi_\alpha^\rho(k)t\right)^s. \end{aligned} \tag{A19}$$

By substitution of $\psi_\alpha^\rho(k)$ (see Equation (4)) into the inner integral we get:

$$\begin{aligned} \int_{-\infty}^{\infty} dk e^{-ikz} \left(\mathcal{D}_\alpha \psi_\alpha^\rho(k)t\right)^s &= \int_{-\infty}^{\infty} dk e^{-ikz} (\mathcal{D}_\alpha (ik)^\alpha \exp[-i\pi\alpha\rho \operatorname{sgn}k]t)^s \\ &= (\mathcal{D}_\alpha t)^s \left(e^{i\pi\alpha\rho s} \int_{-\infty}^0 dk e^{-ikz} (ik)^{\alpha s} + e^{-i\pi\alpha\rho s} \int_0^{\infty} dk e^{-ikz} (ik)^{\alpha s} \right) \\ &= (\mathcal{D}_\alpha t)^s \left(e^{i\pi\alpha\rho s} \int_0^{\infty} dk e^{ikz} (-ik)^{\alpha s} + e^{-i\pi\alpha\rho s} \int_0^{\infty} dk e^{-ikz} (ik)^{\alpha s} \right) \\ &= i \frac{(\mathcal{D}_\alpha t)^s}{z^{1+\alpha s}} \Gamma(1 + \alpha s) \left(e^{i\pi\alpha\rho s} - e^{-i\pi\alpha\rho s} \right) = 2 \frac{(\mathcal{D}_\alpha t)^s}{z^{1+\alpha s}} \Gamma(1 + \alpha s) \sin(-\pi\alpha\rho s). \end{aligned} \tag{A20}$$

Therefore, Equation (A19) reads:

$$\begin{aligned} \frac{1}{2\pi} \int_{-\infty}^{\infty} dk e^{-ikz} \exp\left(-\mathcal{D}_\alpha \psi_\alpha^\rho(k)t\right) &= \frac{1}{2\pi i} \int_{\Omega} ds \Gamma(-s) \Gamma(1 + \alpha s) \frac{\sin(-\pi\alpha\rho s)}{\pi} \frac{(\mathcal{D}_\alpha t)^s}{z^{1+\alpha s}} \\ &= \frac{1}{2\pi i} \int_{\Omega} ds \frac{\Gamma(-s) \Gamma(1 + \alpha s)}{\Gamma(1 + \alpha\rho s) \Gamma(-\alpha\rho s)} \frac{(\mathcal{D}_\alpha t)^s}{z^{1+\alpha s}} = \frac{1}{z} H_{2,2}^{1,1} \left[\frac{\mathcal{D}_\alpha t}{z^\alpha} \mid \begin{matrix} (0, \alpha), (0, \alpha\rho) \\ (0, 1), (0, \alpha\rho) \end{matrix} \right], \end{aligned} \tag{A21}$$

where, in the last equality, we used the Mellin–Barnes integral representation of the Fox H -function (see Equation (A7)). Finally, by using the properties (A11) and (A12), we arrive at:

$$\begin{aligned} \frac{1}{2\pi} \int_{-\infty}^{\infty} dk e^{-ikz} \exp\left(-\mathcal{D}_\alpha \psi_\alpha^\rho(k)t\right) &= \frac{1}{\alpha z} H_{2,2}^{1,1} \left[\frac{z}{(\mathcal{D}_\alpha t)^{1/\alpha}} \mid \begin{matrix} (1, 1/\alpha), (1, \rho) \\ (1, 1), (1, \rho) \end{matrix} \right] \\ &\equiv \frac{1}{(\mathcal{D}_\alpha t)^{1/\alpha}} L_\alpha^\rho \left(\frac{z}{(\mathcal{D}_\alpha t)^{1/\alpha}} \right), \quad 0 < \alpha \leq 2. \end{aligned} \tag{A22}$$

Appendix D. On the Positivity of the q -Order Moments

In this section we show that the moments in Equation (12) are positive if $-1 < q < \alpha$, and $0 < \alpha < 2$. To this end, we distinguish between $0 < \alpha \leq 1$ and $1 < \alpha < 2$.

For $\alpha = 2$, we have $\rho = 1/2$ (see Equation (5)), and the positiveness of fractional-order moments is easily checked. Let us consider $1 < \alpha < 2$, and with the definition of ρ we have $1 - 1/\alpha < \rho < 1/\alpha$. First, we assume $0 < q < \alpha$. Then, together with the variation of ρ we have:

$$\pi q(1 - 1/\alpha) < \pi q\rho < \pi q/\alpha \tag{A23}$$

from where it follows that:

$$0 < \pi q\rho < \pi. \tag{A24}$$

Therefore, we get $\frac{\sin(\pi q \rho)}{\pi q} > 0$. Since $1 - 1/\alpha < 1 - \rho < 1/\alpha$, the same condition holds for $\frac{\sin(\pi q(1-\rho))}{\pi q} > 0$. Now, take $-1 < q < 0$. With the change of variable $r = -q$, we have $0 < r < 1$. With the variation of ρ , we have:

$$-\frac{\pi r}{\alpha} < -\pi r \rho < -\pi r \left(1 - \frac{1}{\alpha}\right), \tag{A25}$$

and with $1 < \alpha < 2$,

$$-\pi r < -\pi r \rho < -\frac{\pi r}{\alpha}, \tag{A26}$$

then, we get $-\pi < \pi q \rho < 0$, which gives $\frac{\sin(\pi q \rho)}{\pi q} > 0$. With the same procedure we get $\frac{\sin(\pi q(1-\rho))}{\pi q} > 0$.

For the case $0 < \alpha \leq 1$, we have $0 < \rho \leq 1$, and, at first, we assume $0 < q < \alpha$. Thus, $0 < \pi q \rho \leq \pi q$, which gives us $0 < \pi q \rho < \pi \alpha \leq \pi$. Hence, $\frac{\sin(\pi q \rho)}{\pi q} \geq 0$, and the same for $\frac{\sin(\pi q(1-\rho))}{\pi q} \geq 0$. Lastly, if $-1 < q < 0$, with the change of variable $r = -q$, we have $0 < r < 1$. With the variation of ρ , we can write:

$$0 < r \rho < 1 \rightarrow -\pi < -\pi r \rho < 0, \tag{A27}$$

which means $\frac{\sin(\pi q \rho)}{\pi q} > 0$. Since $0 < 1 - \rho < 1$, the same condition also holds for $\frac{\sin(\pi q(1-\rho))}{\pi q} > 0$.

Appendix E. Some Details of the Derivation of the First-Arrival Density of Asymmetric Lévy Flights

We start from Equation (17),

$$\begin{aligned} I_1(s) &= \int_{-\infty}^{\infty} dk \frac{1}{s + \mathcal{D}_\alpha \psi_\alpha^\rho(k)} = \int_{-\infty}^0 dk \frac{1}{s + \mathcal{D}_\alpha (ik)^\alpha e^{i\pi\alpha\rho}} + \int_0^{\infty} dk \frac{1}{s + \mathcal{D}_\alpha (ik)^\alpha e^{-i\pi\alpha\rho}} \\ &= \int_0^{\infty} dk \frac{1}{s + \mathcal{D}_\alpha (-ik)^\alpha e^{i\pi\alpha\rho}} + \int_0^{\infty} dk \frac{1}{s + \mathcal{D}_\alpha (ik)^\alpha e^{-i\pi\alpha\rho}}. \end{aligned} \tag{A28}$$

By help of the integral [87],

$$\int_0^{\infty} dx \frac{1}{1+x^\nu} = \frac{\pi}{\nu} \frac{1}{\sin(\pi/\nu)}, \quad \nu > 1 \tag{A29}$$

we obtain:

$$I_1(s) = \frac{\pi}{\alpha} \frac{1}{\sin(\pi/\alpha)} \frac{s^{1/\alpha-1}}{\mathcal{D}_\alpha^{1/\alpha}} \left(ie^{-i\pi\alpha\rho} - ie^{i\pi\alpha\rho}\right) = \frac{2\pi}{\alpha} \frac{s^{1/\alpha-1}}{\mathcal{D}_\alpha^{1/\alpha}} \frac{\sin(\pi\rho)}{\sin(\pi/\alpha)}, \quad \alpha > 1. \tag{A30}$$

Note that for $\alpha \leq 1$, $I_1(s)$ is divergent. For Equation (18) we write:

$$\begin{aligned} I_2(s) &= \int_{-\infty}^{\infty} dk \frac{\exp(ikx_0)}{s + \mathcal{D}_\alpha \psi_\alpha^\rho(k)} = 2\pi \mathcal{F}^{-1} \left[\frac{1}{s + \mathcal{D}_\alpha \psi_\alpha^\rho(k)} \right] (-x_0) \\ &= 2\pi \mathcal{F}^{-1} \left[\mathcal{L} \left[e^{-\mathcal{D}_\alpha \psi_\alpha^\rho(k)t} \right] (s) \right] (-x_0) = 2\pi \mathcal{L} \left[\mathcal{F}^{-1} \left[e^{-\mathcal{D}_\alpha \psi_\alpha^\rho(k)t} \right] (-x_0) \right] (s). \end{aligned} \tag{A31}$$

Recalling Equation (A22), as well as the property $L_\alpha^\rho(-z) = L_\alpha^{1-\rho}(z)$ [72,73], we find:

$$\begin{aligned}
 I_2(s) &= 2\pi \mathcal{L} \left[(\mathcal{D}_\alpha t)^{-1/\alpha} L_\alpha^{1-\rho} \left(\frac{x_0}{(\mathcal{D}_\alpha t)^{1/\alpha}} \right) \right] (s) \\
 &= \frac{2\pi}{\alpha x_0} \int_0^\infty dt e^{-st} H_{2,2}^{1,1} \left[\frac{x_0}{(\mathcal{D}_\alpha t)^{1/\alpha}} \middle| \begin{matrix} (1, 1/\alpha), (1, 1-\rho) \\ (1, 1), (1, 1-\rho) \end{matrix} \right] \\
 &= \frac{2\pi}{\alpha x_0} \int_0^\infty dt e^{-st} H_{2,2}^{1,1} \left[\frac{(\mathcal{D}_\alpha t)^{1/\alpha}}{x_0} \middle| \begin{matrix} (0, 1), (0, 1-\rho) \\ (0, 1/\alpha), (0, 1-\rho) \end{matrix} \right], \tag{A32}
 \end{aligned}$$

where in the last equality, we used Equation (A11). Finally, with the help of Equation (A15), we get:

$$\begin{aligned}
 I_2(s) &= \frac{2\pi}{\alpha x_0} \int_0^\infty dt e^{-st} H_{2,2}^{1,1} \left[\frac{(\mathcal{D}_\alpha t)^{1/\alpha}}{x_0} \middle| \begin{matrix} (0, 1), (0, 1-\rho) \\ (0, 1/\alpha), (0, 1-\rho) \end{matrix} \right] \\
 &= \frac{2\pi}{\alpha x_0} \frac{1}{s} H_{3,2}^{1,2} \left[\frac{\mathcal{D}_\alpha^{1/\alpha}}{x_0} s^{-1/\alpha} \middle| \begin{matrix} (0, 1/\alpha), (0, 1), (0, 1-\rho) \\ (0, 1/\alpha), (0, 1-\rho) \end{matrix} \right]. \tag{A33}
 \end{aligned}$$

With the property (A11), we arrive at the desired result (18). We also mention that $I_2(s)$ for $s = 0$ reads:

$$I_2(0) = \int_{-\infty}^\infty dk \frac{\exp(ikx_0)}{\mathcal{D}_\alpha \psi_\alpha^\rho(k)} = \frac{2}{\mathcal{D}_\alpha x_0^{1-\alpha}} \sin(-\pi\alpha(1+\rho))\Gamma(1-\alpha), \quad \alpha < 1, \tag{A34}$$

which is convergent for $\alpha < 1$. For the limiting case $\alpha = 1$ with $\rho = 1/2$ ($\beta = 0$) we write:

$$\begin{aligned}
 I_1(s) &= \int_{-\infty}^\infty dk \frac{1}{s + \mathcal{D}_1|k|} = 2 \int_0^\infty dk \frac{1}{s + \mathcal{D}_1k} \\
 &= 2 \lim_{a \rightarrow \infty} \int_0^a dk \frac{1}{s + \mathcal{D}_1k} = \frac{2}{\mathcal{D}_1} \lim_{a \rightarrow \infty} \ln(1 + a\mathcal{D}_1/s), \tag{A35}
 \end{aligned}$$

which diverges logarithmically as $a \rightarrow \infty$, and,

$$\begin{aligned}
 I_2(s) &= \int_{-\infty}^\infty dk \frac{\exp(ikx_0)}{s + \mathcal{D}_1|k|} = 2 \int_0^\infty dk \frac{\cos(kx_0)}{s + \mathcal{D}_1k} \\
 &= \frac{2}{\mathcal{D}_1} \sin\left(\frac{sx_0}{\mathcal{D}_1}\right) \int_{\frac{sx_0}{\mathcal{D}_1}}^\infty dz \frac{\sin(z)}{z} + \frac{2}{\mathcal{D}_1} \cos\left(\frac{sx_0}{\mathcal{D}_1}\right) \int_{\frac{sx_0}{\mathcal{D}_1}}^\infty dz \frac{\cos(z)}{z}, \tag{A36}
 \end{aligned}$$

which is convergent for any finite s .

Appendix F. Derivation of the Short-Time and Long-Time Limit of the First-Arrival Density of Asymmetric Lévy Flights

Here, we compute the power-law behaviour of the first-arrival density of asymmetric Lévy flights in the limit of short and long times. For this aim, we first use the Mellin–Barnes integral representation of the two-parametric Mittag–Leffler function (A6) and follow the method in [73] by replacing $\alpha \rightarrow 1$, $\beta \rightarrow 1/\alpha$ and $z \rightarrow \mathcal{D}_\alpha t(ik)^\alpha e^{-i\pi\alpha(1-\rho) \operatorname{sgn}k}$. By applying the inverse Fourier transform we get:

$$\begin{aligned}
 &\frac{1}{2\pi} \int_{-\infty}^\infty dke^{-ikx_0} E_{1,1/\alpha} \left(-\mathcal{D}_\alpha t(ik)^\alpha e^{-i\pi\alpha(1-\rho) \operatorname{sgn}k} \right) \\
 &= \frac{1}{2\pi} \int_{-\infty}^\infty dke^{-ikx_0} \frac{1}{2\pi i} \int_\Omega ds \frac{\Gamma(-s)\Gamma(1+s)}{\Gamma(1/\alpha+s)} \left(\mathcal{D}_\alpha t(ik)^\alpha e^{-i\pi\alpha(1-\rho) \operatorname{sgn}k} \right)^s \\
 &= \frac{1}{2\pi i} \int_\Omega ds \frac{\Gamma(-s)\Gamma(1+s)}{\Gamma(1/\alpha+s)} \frac{1}{2\pi} \int_{-\infty}^\infty dke^{-ikx_0} \left(\mathcal{D}_\alpha t(ik)^\alpha e^{-i\pi\alpha(1-\rho) \operatorname{sgn}k} \right)^s. \tag{A37}
 \end{aligned}$$

Splitting the inner integral into two parts, we find:

$$\begin{aligned} & \int_{-\infty}^{\infty} dk e^{-ikx_0} \left(\Gamma_{\alpha} t (ik)^{\alpha} e^{-i\pi\alpha(1-\rho) \operatorname{sgn}k} \right)^s \\ &= (\Gamma_{\alpha} t)^s \left(\int_{-\infty}^0 dk (ik)^{\alpha s} e^{-ikx_0+i\pi\alpha(1-\rho)s} + \int_0^{\infty} dk (ik)^{\alpha s} e^{-ikx_0-i\pi\alpha(1-\rho)s} \right) \\ &= i \frac{(\Gamma_{\alpha} t)^s}{x_0^{1+\alpha s}} \left(e^{i\pi\alpha(1-\rho)s} - e^{-i\pi\alpha(1-\rho)s} \right) \gamma(1 + \alpha s) = 2 \frac{(\Gamma_{\alpha} t)^s}{x_0^{1+\alpha s}} \sin(\pi(\rho - 1)\alpha s) \gamma(1 + \alpha s). \end{aligned} \tag{A38}$$

Substituting Equation (A38) into Equation (A37) we find:

$$\begin{aligned} & \frac{1}{2\pi} \int_{-\infty}^{\infty} dk e^{-ikx_0} E_{1,1/\alpha} \left(-\mathcal{D}_{\alpha} t (ik)^{\alpha} e^{-i\pi\alpha(1-\rho) \operatorname{sgn}k} \right) \\ &= \frac{1}{2\pi i} \int_{\Omega} ds \frac{\Gamma(-s)\Gamma(1+s)}{\Gamma(1/\alpha+s)} \frac{(\mathcal{D}_{\alpha} t)^s}{\pi x_0^{1+\alpha s}} \sin(\pi(\rho - 1)\alpha s) \Gamma(1 + \alpha s) \\ &= \frac{1}{2\pi i} \int_{\Omega} ds \frac{\Gamma(-s)\Gamma(1+s)\Gamma(1 + \alpha s)}{\Gamma(-\alpha s + \alpha\rho s)\Gamma(1 + \alpha s - \alpha\rho s)\Gamma(1/\alpha + s)} \frac{(\mathcal{D}_{\alpha} t)^s}{x_0^{1+\alpha s}}, \end{aligned} \tag{A39}$$

where, in the last equality, we use Euler’s reflection formula. By comparison with the Mellin–Barnes integral representation (A7) of the Fox H -function, we notice that:

$$\begin{aligned} & \frac{1}{2\pi i} \int_{\Omega} ds \frac{\Gamma(-s)\Gamma(1+s)\Gamma(1 + \alpha s)}{\Gamma(-\alpha s + \alpha\rho s)\Gamma(1 + \alpha s - \alpha\rho s)\Gamma(1/\alpha + s)} \left(\frac{\mathcal{D}_{\alpha} t}{x_0^{\alpha}} \right)^s \\ &= H_{3,3}^{1,2} \left[\frac{\mathcal{D}_{\alpha} t}{x_0^{\alpha}} \middle| \begin{matrix} (0, 1), (0, \alpha), (0, \alpha - \alpha\rho) \\ (0, 1), (0, \alpha - \alpha\rho), (1 - 1/\alpha, 1) \end{matrix} \right]. \end{aligned} \tag{A40}$$

Therefore, in order to obtain the short-time asymptote of the first-arrival density, it is convenient to write Equation (20) in terms of the Mittag–Leffler function,

$$\begin{aligned} \wp_{\text{fa}}(t) &= \frac{\alpha \sin(\pi/\alpha)}{\sin(\pi\rho)} \frac{(\mathcal{D}_{\alpha} t)^{1/\alpha}}{x_0 t} H_{3,3}^{1,2} \left[\frac{\mathcal{D}_{\alpha} t}{x_0^{\alpha}} \middle| \begin{matrix} (0, 1), (0, \alpha), (0, \alpha - \alpha\rho) \\ (0, 1), (0, \alpha - \alpha\rho), (1 - 1/\alpha, 1) \end{matrix} \right] \\ &= \frac{\alpha \sin(\pi/\alpha)}{\sin(\pi\rho)} \frac{(\mathcal{D}_{\alpha} t)^{1/\alpha}}{t} \frac{1}{2\pi} \int_{-\infty}^{\infty} dk e^{-ikx_0} E_{1,1/\alpha} \left(-\mathcal{D}_{\alpha} t (ik)^{\alpha} e^{-i\pi\alpha(1-\rho) \operatorname{sgn}k} \right) \\ &= \frac{\alpha \sin(\pi/\alpha)}{\sin(\pi\rho)} \frac{(\mathcal{D}_{\alpha} t)^{1/\alpha}}{t} \frac{1}{\pi} \left[\int_0^{\infty} dk \cos(kx_0) \operatorname{Re} \left[E_{1,1/\alpha} \left(-\mathcal{D}_{\alpha} t (ik)^{\alpha} e^{-i\pi\alpha(1-\rho)} \right) \right] \right. \\ & \left. + \int_0^{\infty} dk \sin(kx_0) \operatorname{Im} \left[E_{1,1/\alpha} \left(-\mathcal{D}_{\alpha} t (ik)^{\alpha} e^{-i\pi\alpha(1-\rho)} \right) \right] \right]. \end{aligned} \tag{A41}$$

Using the series representation of the Mittag–Leffler function (A5), we find:

$$\begin{aligned} \wp_{\text{fa}}(t) &= \frac{\alpha \sin(\pi/\alpha)}{\sin(\pi\rho)} \frac{(\mathcal{D}_{\alpha} t)^{1/\alpha}}{\pi t} \sum_{n=0}^{\infty} \frac{(-\mathcal{D}_{\alpha} t)^n}{\Gamma(n + \frac{1}{\alpha})} \left\{ \operatorname{Re} \left[i^{n\alpha} e^{-in\pi\alpha(1-\rho)} \right] \int_0^{\infty} dk \cos(kx_0) k^{n\alpha} \right. \\ & \left. + \operatorname{Im} \left[i^{n\alpha} e^{-in\pi\alpha(1-\rho)} \right] \int_0^{\infty} dk \sin(kx_0) k^{n\alpha} \right\} \\ &= \frac{\alpha \sin(\pi/\alpha)}{\sin(\pi\rho)} \frac{(\mathcal{D}_{\alpha} t)^{1/\alpha}}{\pi t} \sum_{n=0}^{\infty} \frac{(-1)^{n+1} (\mathcal{D}_{\alpha} t)^n}{\Gamma(n + \frac{1}{\alpha})} \sin(n\pi\alpha(1 - \rho)) \Gamma(1 + n\alpha) x_0^{-n\alpha-1} \\ &= \frac{\alpha \sin(\pi/\alpha)}{\pi \sin(\pi\rho)} \sum_{n=1}^{\infty} \sin(n\pi\alpha(1 - \rho)) \frac{\Gamma(1 + n\alpha)}{\Gamma(n + \frac{1}{\alpha})} \frac{(-1)^{n+1} \mathcal{D}_{\alpha}^{n+1/\alpha}}{x_0^{n\alpha+1}} t^{n-1+1/\alpha}. \end{aligned} \tag{A42}$$

This expression can also be obtained with the help of Equation (A8).

Another approach to find the long time asymptote of the first-arrival density goes as follows. First, with the help of Equation (A8), we use the series representation of the Laplace transform of the first-arrival density (19),

$$\begin{aligned} \wp_{fa}(s) &= \frac{\mathcal{D}_\alpha^{1/\alpha} \sin(\pi/\alpha)}{x_0 s^{1/\alpha} \sin(\pi\rho)} \\ &\times \left[\sum_{k=0}^\infty \frac{\Gamma(1-\alpha(1+k))\Gamma(1+k)}{\Gamma(\alpha(1-\rho)(1+k))\Gamma(1-\alpha(1-\rho)(1+k))} \frac{\alpha(-1)^k}{k!} \left(\frac{x_0 s^{1/\alpha}}{\mathcal{D}_\alpha^{1/\alpha}}\right)^{\alpha(1+k)} \right. \\ &\left. + \sum_{k=0}^\infty \frac{\Gamma\left(1-\frac{1+k}{\alpha}\right)\Gamma\left(\frac{1+k}{\alpha}\right)}{\Gamma((1-\rho)(1+k))\Gamma(1-(1-\rho)(1+k))} \frac{(-1)^k}{k!} \left(\frac{x_0 s^{1/\alpha}}{\mathcal{D}_\alpha^{1/\alpha}}\right)^{(1+k)} \right]. \end{aligned} \tag{A43}$$

Then, for the small- s asymptote of the Laplace transform, we put $k = 0$ and get:

$$\wp_{fa}(s) \approx 1 - \frac{\sin(\pi\alpha(1-\rho))}{\sin(\pi\rho)} \frac{\Gamma(2-\alpha)}{\Gamma(1/\alpha)\Gamma(2-1/\alpha)} \frac{\mathcal{D}_\alpha^{-1+1/\alpha}}{x_0^{1-\alpha}} s^{1-1/\alpha}. \tag{A44}$$

Then, with the help of the Tauberian theorem [81] (Chapter XIII, Section 5) we find that the small- s asymptote of the Laplace transform,

$$\wp_{fa}(s) \approx 1 - b_2 s^\mu, \quad b_2 = b_1 \Gamma(1-\mu)/\mu, \quad s \rightarrow 0 \tag{A45}$$

corresponds to the long-time asymptote of the PDF ([88], Chapter 3)

$$\wp_{fa}(t) \approx b_1 t^{-1-\mu}, \quad 0 < \mu < 1, \quad b_1 > 0. \tag{A46}$$

Therefore, the resulting long-time asymptote of the first-arrival PDF corresponds to Equation (25).

Appendix G. On the Calculation of the Efficiency for the Limit $\alpha \rightarrow 1$ with $\beta \neq 0$

Let us start from Equation (35) and take $\alpha = 1 + \epsilon$ with $\epsilon > 0$. Then, using $\tan(\frac{\pi}{2} + x) = -\cot(x)$, $\arctan(-x) = -\arctan(x)$, and $\cos(-x) = \cos(x)$, we get:

$$\mathcal{E} = \frac{I_1(\epsilon) \Gamma(\epsilon + 2) K_\alpha}{I_1(\epsilon) x_0^{1+\epsilon}}, \tag{A47}$$

where:

$$I_1(\epsilon) = \sin \left[\frac{\epsilon\pi}{2} + \frac{\epsilon}{1+\epsilon} \arctan \left(\beta \cot \left(\frac{\epsilon\pi}{2} \right) \right) \right], \tag{A48}$$

and:

$$I_2(\epsilon) = \cos \left[\frac{1}{1+\epsilon} \arctan \left(\beta \cot \left(\frac{\epsilon\pi}{2} \right) \right) \right] \cos \left[\arctan \left(\beta \cot \left(\frac{\epsilon\pi}{2} \right) \right) \right]. \tag{A49}$$

Now, we put $\epsilon \rightarrow 0^+$. Then,

$$\cot \left(\frac{\epsilon\pi}{2} \right) = \frac{\cos(\frac{\epsilon\pi}{2})}{\sin(\frac{\epsilon\pi}{2})} = \frac{2}{\epsilon\pi} \left(1 + \mathcal{O}(\epsilon^2) \right), \tag{A50}$$

and since $\arctan(x) \simeq \frac{\pi}{2} - \frac{1}{x} + \dots$ as $x \rightarrow \infty$, we have:

$$\arctan \left[\beta \cot \left(\frac{\epsilon\pi}{2} \right) \right] \simeq \frac{\pi}{2} \left(1 - \frac{\epsilon}{|\beta|} \right) \text{sgn}\beta, \tag{A51}$$

Therefore, Equation (17) becomes:

$$I_1(\epsilon) \underset{\epsilon \rightarrow 0}{\simeq} \sin \left[\frac{\epsilon\pi}{2} + \epsilon(1-\epsilon)\frac{\pi}{2} \left(1 - \frac{\epsilon}{|\beta|} \right) \operatorname{sgn}\beta \right] \\ \simeq \begin{cases} \sin \left(\frac{\epsilon\pi}{2} + \frac{\epsilon\pi}{2} \right) \simeq \epsilon\pi, & \beta > 0 \\ \sin \left(\frac{\epsilon\pi}{2} - \frac{\epsilon\pi}{2} \left(1 - \epsilon - \frac{\epsilon}{|\beta|} \right) \right) \simeq \epsilon^2 \frac{\pi}{2} \left(1 + \frac{1}{|\beta|} \right), & \beta < 0 \end{cases} \quad (\text{A52})$$

Similarly, plugging expression (A51) into (A49) leads us to:

$$I_2(\epsilon) \underset{\epsilon \rightarrow 0}{\simeq} \cos \left[\frac{\pi}{2(1+\epsilon)} \left(1 - \frac{\epsilon}{|\beta|} \right) \right] \cos \left[\frac{\pi}{2} \left(1 - \frac{\epsilon}{|\beta|} \right) \right] \\ \simeq \cos \left[\frac{\pi}{2} (1-\epsilon) \left(1 - \frac{\epsilon}{|\beta|} \right) \right] \sin \left[\frac{\epsilon\pi}{2|\beta|} \right] = \sin \left[\frac{\epsilon\pi}{2} \left(1 + \frac{\epsilon}{|\beta|} \right) \right] \sin \left[\frac{\epsilon\pi}{2|\beta|} \right] \\ \simeq \epsilon^2 \frac{\pi^2}{4} \frac{1}{|\beta|} \left(1 + \frac{1}{|\beta|} \right). \quad (\text{A53})$$

Finally, plugging results (A52) and (A53) into expression (A47), we arrive at Equation (36). We mention that it is also possible to obtain the same solution by using de l'Hôpital's rules for $I_1(\epsilon)$ and $I_2(\epsilon)$.

References

1. Viswanathan, G.M.; Buldyrev, S.V.; Havlin, S.; Da Luz, M.G.E.; Raposo, E.P.; Stanley, H.E. Optimizing the success of random searches. *Nature* **1999**, *401*, 911–914. [CrossRef] [PubMed]
2. Shlesinger, M.F. Search research. *Nature* **2005**, *443*, 281–282. [CrossRef] [PubMed]
3. Bressloff, P.C.; Newby, J.M. Stochastic models of intracellular transport. *Rev. Mod. Phys.* **2013**, *85*, 135. [CrossRef]
4. Luby, M.; Sinclair, A.; Zuckerman, D. Optimal speedup of Las Vegas algorithms. *Inf. Process. Lett.* **1993**, *47*, 173–180. [CrossRef]
5. Gomes, C.P.; Selman, B.; Kautz, H. Boosting combinatorial search through randomization. In Proceedings of the Fifteenth National Conference on Artificial Intelligence (AAAI, 1998), Madison, WI, USA, 26–30 July 1998; Volume 98, p. 431. [CrossRef]
6. Champagne, L.; Carl, R.G.; Hill, R. Search theory, agent-based simulation, and u-boats in the Bay of Biscay. In Proceedings of The 2003 Winter Simulation Conference, Orleans, LA, USA, 7–10 December 2003; p. 991. [CrossRef]
7. Shlesinger, M.F. Random searching. *J. Phys. A Math. Theor.* **2009**, *42*, 434001. [CrossRef]
8. Anderson, J.P.; Stephens, D.W.; Dunbar, S.R. Saltatory search: A theoretical analysis. *Behav. Ecol.* **1997**, *8*, 307–317. [CrossRef]
9. Palyulin, V.V.; Chechkin, A.V.; Metzler, R. Lévy flights do not always optimize random blind search for sparse targets. *Proc. Natl. Acad. Sci. USA* **2014**, *111*, 2931. [CrossRef]
10. James, A.; Pitchford, J.W.; Plank, M.J. Efficient or inaccurate? Analytical and numerical modelling of random search strategies. *Bull. Math. Biol.* **2010**, *72*, 896–913. [CrossRef]
11. Magnello, M.E. Karl Pearson and the establishment of mathematical statistics. *Int. Stat. Rev.* **2009**, *77*, 3. [CrossRef]
12. Shlesinger, M.F.; Klafter, J. Lévy Walks Versus Lévy Flights. In *On Growth and Form*; Stanley, H.E., Ostrowsky, N., Eds.; NATO ASI Series (Series E: Applied Sciences); Springer: Dordrecht, The Netherlands, 1986; Volume 100, pp. 279–283. [CrossRef]
13. Viswanathan, G.M.; Afanasyev, V.; Buldyrev, S.V.; Murphey, E.J.; Prince, P.A.; Stanley, H.E. Lévy flight search patterns of wandering albatrosses. *Nature* **1996**, *381*, 413–415. doi: 10.1038/381413a0 [CrossRef]
14. Viswanathan, G.M.; Da Luz, M.G.; Raposo, E.P.; Stanley, H.E. *The Physics of Foraging: An Introduction to Random Searches and Biological Encounters*; Cambridge University Press: Cambridge, UK, 2011. [CrossRef]
15. Metzler, R.; Klafter, J. The random walk's guide to anomalous diffusion: A fractional dynamics approach. *Phys. Rep.* **2000**, *339*, 1–77. [CrossRef]
16. Ramos-Fernández, G.; Mateos, J.L.; Miramontes, O.; Cocho, G.; Larralde, H.; Ayala-Orozco, B. Lévy walk patterns in the foraging movements of spider monkeys (*Ateles geoffroyi*). *Behav. Ecol. Sociobiol.* **2004**, *55*, 223–230. [CrossRef]
17. Levandowsky, M.; White, B.S.; Schuster, F.L. Random movements of soil amebas. *Acta Protozool.* **1997**, *36*, 237.
18. Mandelbrot, B.B. The Variation of Certain Speculative Prices. *J. Bus.* **1963**, *36*, 394–419. Available online: <https://www.jstor.org/stable/2350970> (accessed on 10 March 2022). [CrossRef]
19. Mandelbrot, B.B. Forecasts of Future Prices, Unbiased Markets and “Martingale” Models. *J. Bus.* **1966**, *39*, 242–255. Available online: <https://www.jstor.org/stable/2351745> (accessed on 10 March 2022). [CrossRef]
20. Carati, A.; Galgani, L.; Pozzi, B. Lévy flights in the Landau-Teller model of molecular collisions. *Phys. Rev. Lett.* **2003**, *90*, 010601. [CrossRef]
21. Chechkin, A.V.; Gonchar, V.Y.; Szydlowsky, M. Fractional kinetics for relaxation and superdiffusion in magnetic field. *Phys. Plasma* **2002**, *9*, 78. [CrossRef]

22. Del-Castillo-Negrete, D. Truncation effects in superdiffusive front propagation with Lévy flights. *Phys. Rev. E* **2009**, *79*, 031120. [[CrossRef](#)]
23. Del-Castillo-Negrete, D.; Carreras, B.A.; Lynch, V.E. Fractional diffusion in plasma turbulence. *Phys. Plasmas* **2004**, *11*, 3854. [[CrossRef](#)]
24. Tribel, O.; Boon, J.P. Lévy Laws for Lattice Gas Automata. In *Pattern Formation and Lattice Gas Automata*; Lawniczak, A., Kapral, R., Eds.; Fields Institute of Mathematics (Toronto): Toronto, ON, Canada, 1994. Available online: <https://citeseerx.ist.psu.edu/viewdoc/download?doi=10.1.1.31.5159&rep=rep1&type=pdf> (accessed on 10 March 2022).
25. Betello, G.; Succi, S. Lévy-flight cellular automata on the IBM RISC-6000 workstation. In Proceedings of the [1991] Proceedings, Advanced Computer Technology, Reliable Systems and Applications, Bologna, Italy, 13–16 May 1991; pp. 695–700. [[CrossRef](#)]
26. Levernier, N.; Textor, J.; Bénichou, O.; Voituriez, R. Inverse Square Lévy Walks are not Optimal Search Strategies for $d \geq 2$. *Phys. Rev. Lett.* **2020**, *124*, 080601. [[CrossRef](#)]
27. Lomholt, M.A.; Koren, T.; Metzler, R.; Klafter, J. Lévy strategies in intermittent search processes are advantageous. *Proc. Natl. Acad. Sci. USA* **2008**, *105*, 11055–11059. [[CrossRef](#)]
28. Palyulin, V.V.; Chechkin, A.V.; Metzler, R. Space-fractional Fokker-Planck equation and optimization of random search processes in the presence of an external bias. *J. Stat. Mech.* **2014**, *2014*, P11031. [[CrossRef](#)]
29. Bénichou, O.; Coppey, M.; Moreau, M.; Suet, P.H.; Voituriez, R. Optimal search strategies for hidden targets. *Phys. Rev. Lett.* **2005**, *94*, 198101. [[CrossRef](#)] [[PubMed](#)]
30. Loverdo, C.; Bénichou, O.; Moreau, M.; Voituriez, R. Enhanced reaction kinetics in biological cells. *Nat. Phys.* **2008**, *4*, 134–137. [[CrossRef](#)]
31. Bartumeus, F.; Levin, S.A. Fractal reorientation clocks: Linking animal behavior to statistical patterns of search. *Proc. Natl. Acad. Sci. USA* **2008**, *105*, 19072–19077. [[CrossRef](#)]
32. Bénichou, O.; Loverdo, C.; Moreau, M.; Voituriez, R. Intermittent search strategies. *Rev. Mod. Phys.* **2011**, *83*, 81. [[CrossRef](#)]
33. Bartumeus, F.; Peters, F.; Pueyo, S.; Marrasé, C.; Catalan, J. Helical Lévy walks: Adjusting searching statistics to resource availability in microzooplankton. *Proc. Natl. Acad. Sci. USA* **2003**, *100*, 12771–12775. [[CrossRef](#)]
34. Pacheco-Cobos, L.; Winterhalder, B.; Cuatianquiz-Lima, C.; Rosetti, M.F.; Hudson, R.; Ross, C.T. Nahua mushroom gatherers use area-restricted search strategies that conform to marginal value theorem predictions. *Proc. Natl. Acad. Sci. USA* **2019**, *116*, 10339–10347. [[CrossRef](#)]
35. Knell, A.S.; Codling, E.A. Classifying area-restricted search (ars) using a partial sum approach. *Theor. Ecol.* **2012**, *5*, 325–339. [[CrossRef](#)]
36. Mooney, B.L.; Corrales, L.R.; Clark, A.E. Molecular networks: An integrated graph theoretic and data mining tool to explore solvent organization in molecular simulation. *J. Comput. Chem.* **2012**, *33*, 853–860. [[CrossRef](#)]
37. Tejedor, V.; Bénichou, O.; Voituriez, R. Global mean first-passage times of random walks on complex networks. *Phys. Rev. E* **2009**, *80*, 065104(R). [[CrossRef](#)] [[PubMed](#)]
38. Perra, N.; Baronchelli, A.; Mocanu, D.; Gonçalves, B.; Pastor-Satorras, R.; Vespignani, A. Random walks and search in time-varying networks. *Phys. Rev. Lett.* **2012**, *109*, 238701. [[CrossRef](#)] [[PubMed](#)]
39. Lomholt, M.A.; Ambjörnsson, T.; Metzler, R. Optimal target search on a fast-folding polymer chain with volume exchange. *Phys. Rev. Lett.* **2005**, *85*, 260603. [[CrossRef](#)] [[PubMed](#)]
40. Reynolds, A.M. Optimal random Lévy-loop searching: New insights into the searching behaviours of central-place foragers. *Europhys. Lett.* **2008**, *82*, 20001. [[CrossRef](#)]
41. Blumenthal, R.M.; Gettoor, R.K.; Ray, D.B. On the distribution of first hits for the symmetric stable processes. *Trans. Amer. Math. Soc.* **1961**, *99*, 540–554. [[CrossRef](#)]
42. Port, S.C. Hitting times and potentials for recurrent stable processes. *J. Anal. Math.* **1967**, *20*, 371–395. [[CrossRef](#)]
43. Port, S.C.; The first hitting distribution of a sphere for symmetric stable processes. *Trans. Amer. Math. Soc.* **1969**, *135*, 115–125. [[CrossRef](#)]
44. Doney, R.A. Hitting probabilities for spectrally positive Lévy processes. *J. Lond. Math. Soc.* **1991**, *44*, 566–576. [[CrossRef](#)]
45. Cordero, F. On the Excursion Theory for the Symmetric Stable Lévy Processes with Index $\alpha \in (1, 2]$ and Some Applications. Ph.D. Thesis, Université Pierre et Marie Curie, Paris, France, 2010. Available online: <http://dml.mathdoc.fr/item/tel-00521136> (accessed on 10 March 2022).
46. Yano, K.; Yano, Y.; Yor, M. *On the Laws of First Hitting Times of Points for One-Dimensional Symmetric Stable Lévy Processes*; Séminaire de Probabilités XLII, 187, Lecture Notes in Math., 1979; Springer: Berlin, Germany, 2009. 8. [[CrossRef](#)]
47. Kwaśnicki, M. Spectral theory for symmetric one-dimensional Lévy processes killed upon hitting the origin. *Electron. J. Probab.* **2012**, *17*, 1–29. [[CrossRef](#)]
48. Juszczyński, T.; Kwaśnicki, M. Hitting times of points for symmetric Lévy processes with completely monotone jumps. *Electron. J. Probab.* **2015**, *20*, 1–24. [[CrossRef](#)]
49. Grzywny, T.; Ryznar, M. Hitting times of points and intervals for symmetric Lévy processes. *Potential Anal.* **2017**, *46*, 739–777. [[CrossRef](#)]
50. Peskir, G. The law of the hitting times to points by a stable Lévy process with no negative jumps. *Electron. Commun. Probab.* **2008**, *13*, 653–659. [[CrossRef](#)]
51. Simon, T. Hitting densities for spectrally positive stable processes. *Stochastics* **2011**, *83*, 203–214. [[CrossRef](#)]

52. Kuznetsov, A.; Kyprianou, A.; Pardo, J.C.; Watson, A. The hitting time of zero for a stable process. *Electron. J. Probab.* **2014**, *19*, 1–26. [CrossRef]
53. Chechkin, A.V.; Metzler, R.; Gonchar, V.Y.; Klafter, J.; Tanatarov, L.V. First passage and arrival time densities for Lévy flights and the failure of the method of images. *J. Phys. A Math. Gen.* **2003**, *36*, L537. [CrossRef]
54. Palyulin, V.V.; Blackburn, G.; Lomholt, M.A.; Watkins, N.W.; Metzler, R.; Klages, R.; Chechkin, A.V. First passage and first hitting times of Lévy flights and Lévy walks. *New J. Phys.* **2019**, *21*, 103028. [CrossRef]
55. Palyulin, V.V.; Chechkin, A.V.; Klages, R.; Metzler, R. Search reliability and search efficiency of combined Lévy-Brownian motion: Long relocations mingled with thorough local exploration. *J. Phys. A Math. Theor.* **2016**, *49*, 394002. [CrossRef]
56. Dybiec, B.; Gudowska-Nowak, E.; Chechkin, A.V. To hit or to pass it over-remarkable transient behaviour of first arrivals and passages for Lévy flights in finite domains. *J. Phys. A Math. Theor.* **2016**, *49*, 504001. [CrossRef]
57. Dybiec, B.; Gudowska-Nowak, E.; Barkai, E.; Dubkov, A.A. Lévy flights versus Lévy walks in bounded domains. *Phys. Rev. E* **2017**, *95*, 052102. [CrossRef]
58. Szu, H.; Hartley, R. Fast simulated annealing. *Phys. Lett. A* **1987**, *122*, 157–162. [CrossRef]
59. Pavlyukevich, I. Lévy flights, non-local search and simulated annealing. *J. Comput. Phys.* **2007**, *226*, 1830–1844. [CrossRef]
60. Pavlyukevich, I. Simulated annealing for Lévy-driven jump-diffusions. *Stochast. Process. Appl.* **2008**, *118*, 1071–1105. [CrossRef]
61. Koren, T.; Chechkin, A.V.; Klafter, J. On the first passage time and leapover properties of Lévy motions. *Phys. A Stat. Mech. Appl.* **2007**, *379*, 10–22. [CrossRef]
62. Koren, T.; Lomholt, M.A.; Chechkin, A.V.; Klafter, J.; Metzler, R. Leapover lengths and first passage time statistics for Lévy flights. *Phys. Rev. Lett.* **2007**, *99*, 160602. [CrossRef] [PubMed]
63. Padash, A.; Chechkin, A.V.; Dybiec, B.; Pavlyukevich, I.; Shokri, B.; Metzler, R. First-passage properties of asymmetric Lévy flights. *J. Phys. A Math. Theor.* **2019**, *52*, 454004. [CrossRef]
64. Padash, A.; Chechkin, A.V.; Dybiec, B.; Magdziarz, M.; Shokri, B.; Metzler, R. First passage time moments of asymmetric Lévy flights. *J. Phys. A Math. Theor.* **2020**, *53*, 275002. [CrossRef]
65. Ditlevsen, P.D. Anomalous jumping in a double-well potential. *Phys. Rev. E* **1999**, *60*, 172. [CrossRef]
66. Chechkin, A.V.; Gonchar, V.Yu.; Klafter, J.; Metzler, R. Barrier crossing of a Lévy flight. *Europhys. Lett.* **2005**, *72*, 348. [CrossRef]
67. Chechkin, A.V.; Sliusarenko, O.Yu.; Klafter, J.; Metzler, R. Barrier crossing driven by Lévy noise: Universality and the Role of Noise Intensity. *Phys. Rev. E* **2007**, *75*, 041101. [CrossRef]
68. Imkeller, P.; Pavlyukevich, I. Lévy flights: transitions and meta-stability. *J. Phys. A Math. Gen.* **2006**, *39*, L237. [CrossRef]
69. Imkeller, P.; Pavlyukevich, I. First Exit Times of SDEs Driven by Stable Lévy Processes. *Stoch. Proc. Appl.* **2006**, *116*, 611–642. Available online: <https://www.sciencedirect.com/science/article/pii/S0304414905001614> (accessed on 10 March 2022). [CrossRef]
70. Dubkov, A.A.; La Cognata, A.; Spagnolo, B. The problem of analytical calculation of barrier crossing characteristics for Lévy flights. *J. Stat. Mech. Theory Exp.* **2009**, *2009*, P01002. [CrossRef]
71. Dubkov, A.A.; Kharcheva, A.A. Features of barrier crossing event for Lévy flights. *EPL (Europhys. Lett.)* **2016**, *113*, 30009. [CrossRef]
72. Zolotarev, V.M. *One-Dimensional Stable Distributions*; American Mathematical Society: Providence, RI, USA, 1986. [CrossRef]
73. Mainardi, F.; Pagnini, G.; Saxena, R.K. Fox H -functions in fractional diffusion. *J. Comput. Appl. Math.* **2005**, *178*, 321–331. [CrossRef]
74. Mainardi, F.; Pagnini, G.; Gorenflo, R. Mellin Transform and Subordination Laws in Fractional Diffusion Processes. *Fract. Calc. Appl. Anal.* **2003**, *6*, 441–459. Available online: <http://www.diogenes.bg/fcaa/volume6/fcaa64/amapago.pdf> (accessed on 10 March 2022).
75. Haubold, H.J.; Mathai, A.M.; Saxena, R.K. Further solutions of fractional reaction-diffusion equations in terms of the H -function. *J. Comput. Appl. Math.* **2011**, *235*, 1311–1316. [CrossRef]
76. Paradisi, P.; Cesari, R.; Mainardi, F.; Maurizi, A.; Tampieri, F. A generalized Fick's law to describe non-local transport effects. *Phys. Chem. Earth Part B Hydrol. Oceans Atmos.* **2001**, *26*, 275. [CrossRef]
77. Paradisi, P.; Cesari, R.; Mainardi, F.; Tampieri, F. The fractional Fick's law for non-local transport processes. *Physica A* **2001**, *293*, 130. [CrossRef]
78. Seshadri, V.; West, B.J. Fractal dimensionality of Lévy processes. *Proc. Natl. Acad. Sci. USA* **1982**, *79*, 4501–4505. [CrossRef]
79. West, B.J.; Seshadri, V. Linear systems with Lévy fluctuations. *Phys. A Stat. Mech. Appl.* **1982**, *113*, 203–216. [CrossRef]
80. Chechkin, A.V.; Gonchar, V.Y. Linear relaxation processes governed by fractional symmetric kinetic equations. *J. Exp. Theor. Phys.* **2000**, *91*, 635–651. [CrossRef]
81. Feller, W. *An Introduction to Probability Theory and Its Applications*, 2nd ed.; Wiley: New York, NY, USA, 1991; Volume 2. Available online: https://www.amazon.de/-/en/William-Feller/dp/0471257095/ref=pd_lpo_1?pd_rd_i=0471257095&psc=1 (accessed on 29 April 2022).
82. Chambers, J.M.; Mallows, C.L.; Stuck, B.W. A Method for Simulating Stable Random Variables. *J. Am. Stat. Assoc.* **1976**, *71*, 340–344. [CrossRef]
83. Palyulin, V.V.; Mantsevich, V.N.; Klages, R.; Metzler, R.; Chechkin, A.V. Comparison of pure and combined search strategies for single and multiple targets. *Eur. Phys. J. B* **2017**, *90*, 170. [CrossRef]
84. Samorodnitsky, G.; Taqqu, M.S. *Stable Non-Gaussian Random Processes: Stochastic Models with Infinite Variance*; Chapman and Hall: New York, NY, USA, 1994. [CrossRef]

85. Prabhakar, T.R. A singular integral equation with a generalized Mittag-Leffler function in the kernel. *Yokohama Math. J.* **1971**, *19*, 7–15.
86. Mathai, A.M.; Saxena, R.K.; Haubold, H.J. *The H-Function: Theory and Applications*; Springer: New York, NY, USA; Dordrecht, The Netherlands; Heidelberg, Germany; London, UK, 2010. [[CrossRef](#)]
87. Prudnikov, A.P.; Brychkov, Y.A.; Marichev, O.I. *Integrals and Series*; Gordon and Breach: New York, NY, USA, 1990.
88. Klafter, J.; Sokolov, I.M. *First Steps in Random Walks*; Oxford University Press: Oxford, UK, 2011. [[CrossRef](#)]